



Historical snowfall measurements in the Central and Southern Apennine Mountains: climatology, variability and trend

Vincenzo Capozzi¹, Francesco Serrapica¹, Armando Rocco¹, Clizia Annella^{2,1}, Giorgio Budillon¹

5 ¹Department of Science and Technology, University of Naples “Parthenope”, Isola C4, CAP 80143, Italy

²Center of Excellence for Telesensing of Environment and Model Prediction of Severe events, University of L’Aquila, L’Aquila, Italy

10

Correspondence to: Vincenzo Capozzi (vincenzo.capozzi@uniparthenope.it)

Abstract. This work presents an analysis of historical snow precipitation data collected in the period 1951-2001 in Central and Southern Apennines (Italy), an area scarcely investigated so far. To pursue this aim, we used the monthly observations of the snow cover duration, number of days with snow and total height of new snow collected at 129 stations located between 288 and 1750 m a.s.l.. Such data have been manually digitized from the Hydrological Yearbooks of the Italian National Hydrological and Mareographic Service. The available dataset has been primarily analyzed to build a reference climatology (related to 1971-2000 period) for the considered Apennine region. More specifically, using a methodology based on Principal Component Analysis and k-means clustering, we have identified different modes of spatial variability, mainly depending from the elevation, which reflect different climatic zones. Subsequently, focusing on the number of days with snow and snow cover duration on the ground, we have carried out a linear trend analysis, employing the Theil-Sen estimator and the Mann-Kendall test. An overall negative tendency has been found for both variables. For clusters including only stations above 1000 m a.s.l., a significant (at 95% confidence level) decreasing trend has been found in winter season (i.e. from December to February): -3.2 [-6.0 to 0.0] days/10 years for snow cover duration and -1.6 [-2.5 to -0.6] days/10 years for number of days with snow. Moreover, in all considered seasons, a clear direct relationship between trend magnitude and elevation has emerged. In addition, using a cross wavelet analysis, we found a close in-phase linkage on decadal time scale between the investigated snow indicators and the Eastern Mediterranean Pattern. For both snow cover duration and number of days with snow, such connection appears to be more relevant in full (i.e. from November to April) and in late (i.e. from February to April) seasons.

1 Introduction

30 In recent years, a great deal of attention has been devoted to the study of past snowfall variability worldwide, mainly in mountain regions. The great interest in this essential climate variable is motivated by several reasons. The snow, in fact, is a pivotal component of the hydrological cycle and exerts, at the same time, a relevant impact on the energy balance, controlling the land surface albedo. In addition, the snow strongly affects the complex ecosystems of mountain areas, as well as the



biogeochemical cycles (e.g. Magnani et al., 2017). Lastly, the occurrence as well as the persistence of snowfall on the ground
35 is decisive for winter tourism and for several economic activities (for instance, hydropower production). Therefore, considering
also the recent climate changes, that are posing serious threats on the cryosphere and mountain regions (e.g. Mote et al., 2018;
Kotlarski et al., 2022), it is crucial to recover and analyse historical long-term time series of snowfall to assess its variability
and tendencies.

In last decades, the satellite observations and the climate model reanalyses have offered new opportunities of build-up snow
40 climatologies worldwide (e.g. Bormann et al., 2018; Olefs et al., 2020), especially in regions in which the availability of in
situ data is scarce or totally absent. However, it should be noted that remote sensing could provide information about snow
cover at an adequate resolution for reliable climatological analyses only for the last 20 years, after the deployment of the
Moderate Resolution Imaging Spectroradiometer (MODIS) constellation (Fugazza et al., 2021). On the other hand, as
highlighted by Vernay et al. (2022), the reliability of reanalyses data can be adversely affected by the low spatial resolution
45 and by the rough representation of several sub-grid processes, such as the orographic precipitation and the local thermal
inversion in mountain valleys. The latter can strongly condition local nivometric regimes, particularly in mountainous areas
characterized by complex orography. For such reasons, despite their well-known weaknesses (Notarnicola, 2020), the ground-
based historical observations can be still considered a cornerstone for studies searching for evidence of past snowfall
variability. Accurate in situ snowfall measures open the chance to analyse in depth the climate change impacts in mountain
50 areas and their relationship with the altitude, especially when they can be coupled with high quality and homogenized
temperature and total precipitation measurements (Beaumet et al., 2021). In addition, the ground observations can be
considered an invaluable benchmark to validate satellite and modelled snow data.

In the large body of available scientific literature, snow and snow cover have been investigated employing different parameters,
namely the snow depth (hereafter, HS), the height of new snow (hereafter, HN), the snow water equivalent, the snow cover
55 area, the snow cover duration (hereafter, SCD) and the number of days with snow (hereafter, NDS).

Focusing on the Central Mediterranean area, which can be considered a key-area for study of climate changes mainly due its
complex meteorological regime and to its challenging topography, a lot of research has been paid to the Alpine region (Marty,
2008; Terzago et al., 2010; Valt and Ciafarra, 2010; Marty and Blanchet, 2012; Scherrer et al., 2013; Terzago et al., 2013;
Marcolini et al., 2017b; Matiu et al., 2021; Bertoldi et al., 2023). In this area, in fact, there is a great availability of snowfall
60 climatological time series, some of them stretching back to the late 18th century (Leporati and Mercalli, 1994). Although it is
clear challenging to draw a coherent picture regarding changes in Alpine nivometric regimes, since trends direction and
significance are highly dependent on the considered time period, a general decreasing tendency has been found for SCD in the
period 1972-2006 (Bartolini et al., 2010) as well as in HS for the period 1971-2019 (Matiu et al., 2021).

The Apennine region, despite having a good heritage of old snowfall data, has been poorly investigated up to now. The peer-
65 reviewed literature for this area counts only few recent works (Petriccione and Bricca, 2019; Diodato et al., 2022; Capozzi et
al., 2022; Annella et al., 2023), which presented evidence based on a single or few climatological time series. These studies
highlighted a general negative tendency in snowfall for different indicators, except for the last 20 years, in which a recovery



of SCD, HN and NDS has been detected in the Southern Apennines (Capozzi et al., 2022; Annella et al., 2023). Other interesting results have been provided by two reports (Fazzini et al., 2006; Fazzini, 2007) published in the official information magazine of the Interregional Association for coordination and documentation of snow and avalanche problems (70 <https://aineva.it/en/neve-e-valanghe-magazine/>, last access on 16/01/2024). More specifically, Fazzini et al. (2006) analysed the 1982-2004 period, finding, for the Apennines area, a marked spatial heterogeneity in HN, SCD and NDS trends. From this study, in fact, emerged a strong positive tendency for the investigated variables in the Northern Apennines (eastern sector), a negligible trend in Central Apennines and local positive tendencies in the southern sector. Fazzini (2007) has obtained a similar result for the number of days with HN > 5 cm. (75

The peripheral attention dedicated to the Apennines can be mainly attributed to the very fragmented management of the meteorological monitoring network, which resulted into a non-uniform spatial and temporal coverage of snowfall data. Historically, the snowfall monitoring in the Apennines areas has been handled by the Italian National Hydrological and Mareographic Service (hereafter, NHMS). The latter managed the hydro-meteorological data collection in Italy from 1917 to (80 2002 and was structured into 14 different compartments (Parma, Venezia, Genova, Bologna, Pisa, Rome, Pescara, Naples, Bari, Catanzaro, Palermo, Cagliari, Trento and Bolzano), defined based on the water catchment areas of the main Italian rivers. The NHMS snowfall dataset is currently not available into an easily accessible digitized format and, therefore, it has been largely unexploited so far.

After the disposal of NHMS, whose competences were transferred to the local regional agencies according to the new (85 Legislative Decree issued by Italian government, many historical stations were dismissed or relocated. Unfortunately, the monitoring of snowfall precipitation was interrupted, except in few areas, mainly in the Emilia-Romagna and in Abruzzo regions, where automatic nivometric stations have been progressively installed (Tecilla, 2007). Additional contributions to the snowfall monitoring in Apennines Regions came from the Meteomont Service, which is managed by the Italian Arm of Carabineers, and from the Meteorological Service of the Italian Air Force (hereafter, MSIAF). The Meteomont network started (90 in 1980s for avalanches danger assessment on synoptic/regional scale and actually consists, for Apennines, of 84 manual stations and 2 high altitude surveys (<https://meteomont.carabinieri.it/stazioni-manuali?lang=en>, last access on 04/01/2024). The data collected by such stations are publicly available in a digitized format through the Meteomont website (<https://meteomont.carabinieri.it/archivio-condizioni-meteonivologiche?lang=en>, last access on 04/01/2024). However, most of the time series are strongly incomplete and, therefore, their use for climatological purposes is challenging or prohibitive. (95 The MSIAF snowfall measurements are available since 1981 for 80 monitoring sites and consist of daily observations of HS and of three-hourly measurements of the equivalent liquid water of the accumulated snowfall (Fazzini et al., 2006). The entire Apennines region is monitored by MSIAF network through 15 stations, having an altitude between 352 and 2165 m above sea level (hereafter, a.s.l.). However, such data are not publicly accessible and, more importantly, are strongly unevenly distributed in space and altitude, so they are not suitable for a reliable climatological characterization of the Apennines region.

(100 In the light of this state of the art, a relevant lack of research exists in the knowledge of past snowfall variability in the Apennines. This work aims to provide a contribution to fill this gap, through the rescue of 281 historical time series of snowfall



data collected by NHMS network in an area including a large part of the Central Apennines and a small sector of the Southern Apennines. After a careful quality control, a complete and high-quality dataset consisting of 110 and 114 monthly time series of SCD and NDS, respectively, collected during the period 1951-2001 and of 120 monthly time series of HN measured in the 1971-2001 period has been obtained. This dataset has been adopted to accomplish the two main goals of this study:

- Building-up an updated and solid reference climatology for SCD, NDS and HN variables (related to 1971-2000 period) for the considered Apennine region.
- Providing new evidence about long-term tendencies in NDS and SCD for the study area, analysing their relationship with the elevation.

The remainder of the paper is organized as follows: Section 2 describes the study area, the data and the methods, Section 3 presents the results, Section 4 is dedicated to the discussions and, finally, Section 5 provides the conclusions.

2 Materials and methods

2.1 Study area

The Apennines Mountains consist of parallel mountain ranges extending for about 1200 km from northwest to southwest along the length of the Italian Peninsula. They are conventionally subdivided into three different sectors: the northern sector, including the Ligurian and the Tuscan-Emilian Apennines, the central sector, encompassing the Umbria-Marche Apennines and the Abruzzi Apennines, and the southern sector, comprising the Samnite and Campania Apennines, the Lucan Apennines and the Calabria and Sicily Apennines. In this study, we focused on a study region embracing a large portion of the Central Apennines and a small sector of the Southern ones (Fig. 1). This area extends from 40.5 to 43.5°N in latitude and from 12.5 to 16.0°E in longitude and includes the following Italian administrative regions: Umbria, Lazio, Abruzzo, Molise, Campania, Puglia and Basilicata. It has a very complex orography, consisting of several mountain ranges. The main orographic features, highlighted by filled-in brown triangles in Fig. 1, are (from north to south): the Sibillini mountains (2476 m a.s.l.), the Laga mountains (2458 m a.s.l.), the Reatini mountains (2217 m a.s.l.), the Gran Sasso area (2912 m a.s.l.), the Sirente-Velino mountains (2487 m a.s.l.), the Majella massif (2793 m a.s.l.), the Marsicani mountains (2285 m a.s.l.), the Matese massif (2050 m a.s.l.), the Partenio (1598 m a.s.l.), the Picentini mountains (1809 m a.s.l.) and the Vulture-Li Foj area (1365 m a.s.l.). Moreover, the study area also includes several Apennine offshoots, marked as filled-in green triangles in Fig. 1, such as the Lazio Sub-Apennines (2063 m a.s.l.), the Daunian mountains (1132 m a.s.l.), the Gargano massif (1065 m a.s.l.), and the Murge plateau (686 m a.s.l.). The study region is bounded by flat areas which gradually slope down to the Tyrrhenian Sea (to the west) and to the Adriatic Sea (to the east).

The climate of this area presents distinct Mediterranean features, with a precipitation maximum between late autumn and mid-winter and a relevant minimum in mid-summer. According to Crespi et al. (2018), the spatial distribution of the accumulated precipitation is strongly conditioned by the orography of the region and exhibits a marked west-to-east gradient, with drier



conditions along the Adriatic sector. It is interesting highlighting that, on average, the highest annual precipitation amounts
135 (up to 2200-2500 mm) are observed in the massifs of the Southern Apennines, i.e. in the Matese, Partenio and Picentini areas.
Although they have a lower altitude than the mountains of the Central Apennines, such reliefs lie in a relatively less-complex
orographic context and, therefore, they receive precipitation by a wide spectrum of synoptic patterns (Capozzi et al., 2022).
Regarding the snowfall precipitation, the only climatological reference is the old study of Gazzolo and Pinna (1973). This
work provided a coarse climatology for the HN, SCD and NDS parameters for the whole Italian Peninsula, using the data
140 collected by NHMS during the 1921-1960 period. According to Gazzolo and Pinna (1973), the major peaks of the Central
Apennines (Gran Sasso, Sibillini, Laga Mountains and Majella) received, in the considered time interval, up to 400 cm of fresh
snow per year. In the mountainous areas of the Southern sector (Matese, Partenio and Picentini), the average total yearly HN
is slight above 200 cm. In contrast to what is generally observed for the total precipitation, the snowfall amounts observed in
the eastern slopes of the Central Apennines and in adjacent flat and coastal areas are higher than those measured in the western
145 sectors. This can be related to the effects of the cold continental air masses coming from Balkan region and Eastern Europe,
which stimulate abundant snowfall precipitation through two main mechanisms: the vertical transport of moisture and heat
connected to their passage over the Adriatic Sea, and the orographic forcing, which is related to their interaction with the
mountain ranges. Regarding the SCD, the yearly climatological value is between 50 and 100 days (or greater) in the main
reliefs of the Central Apennines, whereas it is generally below 50 days in the Southern massifs. The frequency of occurrence
150 of snowfall events is very high (25-50 days) in the Central sector, while, according to Gazzolo and Pinna (1973) it is lower
than 20 days in the Southern areas.

The mean annual temperature exhibits a strong altitudinal gradient, decreasing from the 16-17°C of the coastal areas to the 13-
14°C of the base of Apennines and, finally, to the 2-4°C of the highest peaks of the Central sector (Curci et al., 2021). As
perfectly testified by the climatology presented in Brunetti et al. (2014), the valleys and the sub-mountain areas of the Abruzzo
155 region have a mean annual temperature lower than the most of hilly regions of Campania, Puglia and Molise. This difference
is mainly due to the minimum temperature (Curci et al., 2021) and can be ascribed to the frequent occurrence, in the Abruzzo
valleys, of the thermal inversion phenomenon.

2.2 Data rescue

In this study, we have exploited the database of four NHMS compartments: Naples, Bari, Rome and Pescara. The data collected
160 by the stations belonging to the NHMS network were published in the Hydrological Yearbooks, which are freely accessible in
printed version (i.e. as scanned images in portable document format) through the Italian Institute for Environmental Protection
and Research (ISPRA) website (<http://www.bio.isprambiente.it/annalipdf/>, last access on 09 January 2024). The editing and
the publishing of the Hydrological Yearbooks were handled by the Departmental Office of the NHMS responsible for a specific
compartment. Each Hydrological Yearbook contains the data collected in a certain year and was generally structured in two
165 different parts: the Part I, which includes the thermometric and pluviometric measurements and the Part II, which contains a
wide spectrum of data, related to precipitation, hydrology, groundwater levels, exceptional events and tide measurements

(<https://www.isprambiente.gov.it/en/projects/inland-waters-and-marine-waters/hydrological-yearbooks>, last access on 09 January 2024). The snowfall data are included in the Part II of the Hydrological Yearbooks from 1917 to 1934 and in the Part I from 1935 onwards.

170 More specifically, the snowfall data are reported for October to May period and consist of the following parameters: SCD, NDS, HS and HN. From 1917 to 1934, the available measurements include the daily HN, the corresponding snow-to-liquid equivalent amount, the monthly NDS value and the HS value before the occurrence of a determined snowfall event. Subsequently, the snowfall data are reported with a different format. Regarding the SCD and NDS parameters, monthly data are available from 1935 to 1999 for Naples and Rome compartments, from 1935 to 2000 for Bari compartment and from 1935
175 to 2013 for Pescara compartment. The temporal coverage of HS data resembles the one of SCD and NDS; however, it should be highlighted that for this parameter only three daily observations per months (at the end of each decade) are available from 1935 to 1971 and only one (in the last day of a determined month) in the subsequent periods. As concerns the HN variable, unfortunately no data are available from 1935 to 1970, whereas monthly observations are reported from 1971. The snowfall measurements have been manually performed using a traditional nivometer, consisting of a snowboard and a graduated
180 yardstick (De Bellis et al., 2010). It is important to highlight that according to the NHMS standard, the monitored snowfall parameters are defined as follows:

- SCD is the total number of days in a given month or in a given season with snow depth on the ground ≥ 1 cm.
- NDS is the total number of days in a given month or in a given season on which the accumulated snowfall (i.e. the amount of fresh snow with respect to the previous observations) is at least 1 cm.
- 185 • HN is the daily or monthly amount of fresh snow (expressed in cm). The monthly value is intended as the sum of daily HN data observed in a determined month.
- HS is the daily snow depth on the ground (expressed in cm).

From 1917 to the end of 1940s, the data availability is limited and is strongly conditioned by the First and Second World Wars
190 period (in which many stations temporarily interrupted their monitoring activity). The number of stations reporting snowfall data increased in the early 1950s and it was fairly stable until the end of 1990s except for some isolated drops (in 1989 and in 1997). Subsequently, after the closure of NHMS, the data availability strongly decreased and was restricted to some stations of the Abruzzo region, which continued to collect snowfall data under the management of local regional authorities, and to the Montevergine Observatory station (Southern Apennines), which autonomously continued the meteorological parameters
195 recording (Capozzi et al., 2020).

In this study, we decided considering the 1951-2001 period, which corresponds to the years with the highest number of data. More specifically, we have digitized the SCD, NDS, HN and HS data collected by stations having an elevation greater than 250 m a.s.l.. In other words, we have excluded the stations located in flat areas or along the coasts, in which the occurrence of snowfall is relatively rare. Using this criterion, we have retrieved 281 stations, having an elevation ranging between 288 and
200 2125 m a.s.l.. Note that for the digitization process we have used a simply “key-entry” method. Despite the recent introduction



of new approaches and methodologies based on the optical character recognition software and machine learning tools, the manual transcription is still the most accurate technique for climate data digitization. As shown by Brönnimann et al. (2006), the manual method has the lower error rate and well fits the recommendations and the standards practises of the World Meteorological Organization (WMO, 2016), although it is the slower in terms of amount of rescued data per unit of time. The digital templates have been developed in Microsoft Excel and have been structured into different spreadsheets, one dedicated to the station metadata and the other ones to the data of the available snowfall parameters.

A complete list of all rescued stations, with details about geographical coordinates (latitude, longitude and height a.s.l.), membership NHMS compartment and percentage of available data, is provided in the Supplementary material.

210 **2.3 Data, quality control and homogenization**

In this work, we have analysed the SCD and NDS data collected in the 1951-2001 period and the HN data measured between 1971 and 2001. We have decided not to consider the HS data: the latter, in fact, have been reported in the Hydrological Yearbooks with a format, consisting in three or one daily observations per month, which is not suitable for a reliable climatological analysis.

215 Fig. 2 presents the histograms of the data availability for three considered parameters, SCD (Fig. 2a), NDS (Fig. 2b) and HN (Fig. 2c). The data availability has a clear bimodal distribution, with two distinct peaks, one between 0 and 10% and the other between 85 and 100%. From a simple visual inspection of Fig. 2, it emerges that a non-negligible fraction of the rescued stations has a limited data availability. For SCD and NDS (HN), the 39% (37%) of the measuring stations has a data availability less than 50%. According to the criteria suggested by the World Meteorological Organization (WMO, 2008), we have discarded the stations with less than 80% of the available data in the observation period. Moreover, we have rejected some stations belonging to the Rome compartment, namely Abeto, Castelluccio di Norcia, Monte Terminillo (only for SCD and NDS) and Bagnara (only for SCD), due to the presence of many suspicious records. This screening yielded a subset consisting of 129 stations, whose position is shown in Fig. 3a. The spatial distribution of the stations is quite uniform over the entire region, except for the northern side (Umbria-Marche Apennines): for this area, there are only four stations located at an altitude ranging between 529 and 750 m a.s.l.. The density of stations is particularly high in the proximity of the main mountain ridges of Abruzzi and Samnite Apennines. In the Southern sectors, only one station (Montevergine Observatory) is located above 1000 m a.s.l.. Regarding the elevation distribution, which is sketched in Fig. 3b, a relevant number of stations (69) is between 600 and 900 m a.s.l., 27 stations are below 600 m a.s.l. and the remaining (33) are above 900 m a.s.l.; the elevation ranges from a minimum of 288 m to a maximum of 1750 m a.s.l..

230 The considered dataset has been subjected to an accurate quality control (hereafter, QC). It is widely known, in fact, that the quality assurance of climate data is crucial to improve the confidence in any further analysis. As pointed out in many papers, the reliability and the consistency of an historical climatological time series can be affected by several artefacts and errors,



caused by instruments failures, human mistakes in data collection and inaccuracies in the digitization of paper-based data. In this study, we have developed a QC strategy consisting of three statistical tests:

- 235
- The gross error test, which flags the data that are above or below acceptable physical limits;
 - The consistency test, which involves an inter-variable check;
 - The tolerance test, which is focused on the outlier detection.

Note that this QC strategy has been applied to the monthly SCD and NDS time series available in the 1951-2001 period and to the monthly HN time series available in the 1971-2001 time segment.

240 The gross error test aims to identify the clearly erroneous values and consists of comparing the monthly SCD, NDS and HN values to their physical limits. For SCD, we have checked for cases in which, for a determined month and for a certain station, the number of days with snow on the ground is greater than the number of days in that month (e.g. SCD is 32 days in January). For NDS, we have applied a very similar criterion, flagging as “gross errors” the circumstances in which the NDS value is equal or greater than the number of days in a determined month. According to this criterion, the instance in which a new snow
245 event occurred in every day of a certain month is considered an implausible situation. For monthly HN values, we have considered the limit (500 cm) recommended by WMO (2008).

The second step of the QC process aims to detect inconsistencies between pairs of the investigated variables. More specifically, the purposes of this test is to detect the following instances: i) the NDS value for a determined month and a certain station is greater than the SCD value; ii) the NDS value for a determined month and a certain station is zero and the HN value is greater
250 than zero; iii) the NDS value for a certain month and a determined station is greater than zero and the NH value is null. By applying the gross and the consistency checks, 1527 monthly invalid data were found: in particular, the 2.0% of the erroneous data emerged from the gross test, whereas the remaining 98.0% represents the outcome of the consistency test. A relevant fraction of the bad data can be attributed to instances in which the NDS value is greater than the SCD value. In some Hydrological Yearbooks, in fact, the NDS value is reported in the column dedicated to the SCD value and vice versa. Therefore,
255 in most of the cases, the identified errors have been easily corrected; in other circumstances, they have discarded and replaced with a missing data marker.

The tolerance test has been performed using the Climatol method. The latter has been developed by Guijarro (2018) and is widely employed for the QC, homogenization and in filling of the missing data for a set of climatological time series. The Climatol data processing starts with a normalization of the original data. In this respect, Climatol offers different approaches
260 for normalization, depending on the climatological variable. In this study, the type of normalization (*std*) has been set to 1 (which means that data normalization is based on deviations from mean) for SCD and NDS, whereas we selected *std* = 2 (which means normalize using ratio to normal climatological value) for HN. The approach used by Climatol to detect outliers is inspired by the principles of the spatial consistency check. In particular, for any candidate time series, this method use data from neighbouring stations to generate a composite reference series. In the default settings of the Toolbox, the vertical and
265 horizontal distances between a suitable reference series and the candidate one have the same weight. Following Buchmann et al. (2022), in this study we have adjusted the scale parameter of the vertical coordinate (*wz*) so that the elevation counts 100



time more; in other words, the approach used in our work means that an altitude difference of 500 m corresponds to a horizontal distance of 50 km. The reference series is used to create time series of anomalies by subtracting the estimated values from the observed ones. The values of the anomalies time series that exceed a determined threshold (dz_{max}) are labelled as outliers and are discarded. More specifically, the dz_{max} value, set by default to ± 5 standard deviations, was properly tuned to ensure that the flagged outlying values were not rejected because of their extremeness. After several sensitivity experiments, in which we manually inspected the data flagged as potential outliers, the dz_{max} parameter has been set as follows: $dz_{max} = 15$ for SCD and NDS and $dz_{max} = 20$ for HN. Using this criterion, the tolerance test flagged as outliers only two NDS monthly observations, related to Frigento and Roccasicura time series.

Climatol has been employed in this study also to check for homogeneity of the investigated time series. The use of this toolbox for the homogenisation of snowfall data has been explored, with encouraging results, in some recent works (Buchmann et al., 2022; Buchmann et al., 2023). As described in detail by Guijarro (2018) and by Kuya et al. (2022), the Climatol homogenization method is based on the Standard Normal Homogeneity Test (SNHT; Alexandersson, 1986) for the identification of the breaks and on a linear regression approach for the adjustments (Easterling and Peterson, 1995). The SNHT is applied to the anomalies time series previously introduced in the description of the tolerance test. In brief, the Climatol homogenization process is structured in two procedures. In the first one, called “stepped overlapping windows”, the toolbox computes the SNHT test for all series, retaining the maximum SNHT value for each series. The series having a maximum SNHT value greater than a specific threshold ($snht1$) are split into two subseries at the point of the maximum SNHT value. Subsequently, the sub-series are tested again and the procedure is iterated until the maximum SNHT value of the sub-series is below the $snht1$ threshold. After this procedure, the test is applied to the whole series in order to detect further breaks, using a threshold value $snht2$. Once detected a break for a determinate candidate time series, the latter is corrected back in time starting from the most recent homogeneous time interval. The break magnitude corrections are computed as the variation of the mean before and after homogenisation procedure. Additional details about the calculation of the adjustment factor can be found in Guijarro (2018), in Kuya et al. (2022) and in Buchmann et al. (2023). The last step of Climatol processing consists in the filling of all missing values using the weighted ratios of neighbouring series and in the production of the final high quality, homogeneous and complete time series. It is important highlighting that Climatol offers the opportunity to carry out a first explanatory analysis of the data, which is very useful for the tuning of several parameters, including $snht1$ and $snht2$. The main settings adopted to run Climatol for tolerance test of QC and homogenization are listed in Table 1.

Using this set-up, Climatol flagged as inhomogeneous seven SCD and two NDS time series. Details about date in which the breaks occurred and the corresponding value of SNHT are supplied in the Supplementary Material. From a visual inspection of such time series, the results of the homogeneity test seemed very reasonable. The identified breaks were further examined against the metadata reported on the Hydrological Yearbooks. However, the latter contain only few useful information, that allowed to verify only if the stations were relocated (this is not the case for any of the stations identified as inhomogeneous). We therefore do not have enough information to determine the cause of the inhomogeneities. We decided to adopt a precautionary approach and, therefore, the detected breaks were accepted.



2.4 Cluster analysis

In order to building up a reference climatology for the three parameters investigated in this study, the SCD, NDS and HN time series have been grouped into different clusters, each representing a specific climatic zone. Following the previous literature, we used a multivariate method based on the Principal Component Analysis (PCA) and Cluster Analysis (CA). This approach has been employed in different areas (Kidson, 1994; Sumner et al., 1995; Frago and Tildes Gomes, 2008; Capozzi et al., 2023), proving to be reliable in the classification of meteorological data.

To search for relationships between the available time series, the (non-rotated) PCA has been applied in S-mode to a dataset consisting of n «observations» (i.e. the stations, 110 for SCD, 114 for NDS and 120 for HN) and m «variables» (i.e. the monthly data, 612 for SCD and NDS and 372 for HN). It is important highlighting that the PCA has been employed not as a merely data reduction technique, but as a method which guarantees that only the fundamental modes of variation of the data are taken into account. Using the scree plot, we have determined the appropriate number of principal components (PCs) for each of the three investigated parameters. After this pre-processing, the well-known non-hierarchical k-means method (Anderberg, 1973) was then performed using the selected PCs as input. This means that sites with similar loadings on the extracted PCs have been clustered together. In the selection of the optimal number of clusters, we searched for the best trade-off between subjective evaluation, based on the patterns expected from the climatic and topographic drivers, and the semi-objective metrics («elbow method»).

2.5 Statistical analyses

In order to evaluate the magnitude of the trend slope in SCD and NDS time series, the well-known Theil-Sen non-parametric test was employed (Sen, 1968). This procedure is largely used in the hydro-meteorological framework because of its robustness in the presence of outliers in the series (Song et al., 2015; Bartolomeu et al., 2016; Ortiz-Gomez et al., 2020). To assess the trend magnitude, the Theil-Sen procedure estimates the trend slope in a determined sample for all data pairs. The median of all samples computed for each data pairs coincides with steepness of the trend. On the other hand, the statistical significance was assessed with the Mann-Kendall non-parametric test (Mann, 1945; Kendall, 1962). This test is a rank-based method for assessing the presence of increasing or decreasing monotonic trends in time series data and it is often used because of its property of requiring minimal assumptions about the data that need to be tested (Hamed, 2008). The significance levels of 0.05 and 0.1 (i.e., the 95% and 90% confidence levels, respectively) have been used to test the null hypothesis that there is no trend in the data. It is important to highlight that prior to the application of these statistical tests, the pre-whitening technique was used to reduce the effect of lag-one autocorrelation in the analyzed time series (e.g. Caloiero et al., 2011, Trambly et al. 2013). In addition, to measure the relationship between the linear trend of the analysed parameters and the elevation, we employed the traditional Pearson correlation coefficient (hereafter, ρ).



2.6 Wavelet analysis

The Wavelet analysis is a very appealing alternative to the classic short time Fourier Transform for the geophysical time series analysis and periodicities examination. The Wavelet tool, in fact, allows discriminating not only the main frequencies in a non-stationary series, but also localizing them in time (Percival, 2008). This is a very useful feature for the analysis of climate data, whose variability is typically modulated by nonstationary processes. Because of such remarkable advantages, we have decided to apply the Wavelet Transform (WT) to the clustered-averaged SCD and NDS time series involved in this study to identify their oscillation in the frequency domain. Among the main WT categories (Grinsted et al., 2004), we have chosen the Continuous Wavelet Transform (CWT), which is particularly suitable for the analysis of scale and time-dependant features of a time series. The CWT searches for a similarity between the investigated signals and a well-known mathematical function (the wavelet). The latter is applied several times with different scales to the considered time series and at different temporal locations. Similarly to other studies (e.g. Carey et al., 2013; Marcolini et al., 2017b), we have decided to apply the Morlet function as wavelet function. Additional details about the mathematical formulation of this function as well as about the wavelet analysis and the methods used to assess the statistical significance of the power spectrum can be found in Grinsted et al. (2004). It is important highlighting that CWT presents some deficiencies at the edges of the investigated time series. Therefore, it is useful to introduce a cone of influence, where the results are uncertain (Torrence and Compo, 1998). The CWTs of two signals can be combined to obtain the Cross Wavelet Transform (XWT), which offers the possibility to detected the areas, in the time-frequency domain, where the two CWTs share common features in terms of power and relative phase (for mathematical details, see Grinsted et al., 2004).

3 Results

3.1 Regionalization

The PCA of monthly SCD, NDS and HN time series allowed extracting the essential modes of spatial variability. According to the evidence provided by the scree plot, we have considered the first four PCs for SCD (which account for the 73% of the total variance), the first nine PCs for NDS (which explain the 70% of the total variance) and the first four for the HN (which account for the 70% of the total variance). Such levels of explained variance seem to be acceptable, given the considerable number of stations and the complex nature of the snowfall variables. It is interesting highlighting that, in all three cases, the first PC explains most of the variance (61.2% for SCD, 51.8% for HN and 47.7% for NDS). From the analysis of PC loadings, which can be regarded as the correlation of the original series with the principal component, it clearly emerges that the first PC reflects the altitude-related variability of the three snowfall indicators across the whole elevation range. The other considered PCs explain a very limited portion of variance (generally ranging between 1 and 8%) and are linked with the



difference between eastern and western sides of the Apennines, the distance from the sea, the hours of direct sunlight (which is connected with the third PC of the SCD) and with local patterns strongly conditioned by the orography.

365 The PCA loadings from the selected PCs were employed as input of the k-means algorithm. After several tests and sensitivity analysis to assess cluster reproducibility and stability, four clusters were chosen for SCD and NDS and three for HN. The clustering of the available stations based on monthly SCD, NDS and HN data is presented in Fig. 4. From a visual inspection of this figure, as well as of Table 2, it is straightforward notice that the clusters are relatively well separated in altitude. Starting from SCD (Fig. 4a), the identified groups are populated by a number of stations that is inversely proportional to the median
370 elevation. More specifically, as revealed by Table 2, the cluster 1 comprises 58 stations and has a median altitude of 648 m a.s.l. (min-max: 288-910 m a.s.l.); the cluster 2 counts 26 stations having a median elevation of 815 m a.s.l. (min-max: 550-954 m a.s.l.); the cluster 3 includes 14 stations and has a median elevation of 1000 m a.s.l. (min-max: 750-1157 m a.s.l.), and, finally, cluster 4 includes 12 stations having an altitude greater or equal to 1000 m a.s.l. (median value: 1290 m a.s.l.). The altitudinal range of the stations is around 400 m for all clusters, except the cluster 1. The latter, in fact, includes not only low-
375 elevation sites but also stations located on eastern and southern mountain slopes of the Central Apennines chain, which are located in topographic contexts unfavourable to the persistence of snow on the ground due to the high number of hours of direct sunlight.

The four groups emerged from the clustering of NDS data are shown in Fig. 4b. According to Table 2, most of the stations are nearly equally distributed among the first three clusters (31 belong to cluster 1, 34 to cluster 2 and 35 to cluster 3). The cluster
380 1 includes low-elevation sites (median altitude 569 m a.s.l., min-max: 288-850 m a.s.l.) and stations located in the main valleys of Abruzzo region. The second cluster has a slight higher median elevation (700 m a.s.l., min-max: 520-910 m a.s.l.) and brings together a relevant number of hilly sites of the Southern and Samnite Apennines, as well as several stations located on the eastern side of Majella mountains. The stations belonging to the third cluster span a significant altitudinal range (from 650 to 1375 m a.s.l.) and have a median elevation of 879 m a.s.l.. The fourth cluster is very similar to the SCD cluster 4: it includes,
385 in fact, only high-elevation sites having a median elevation of 1220 m a.s.l. (min-max: 1000-1430 m a.s.l.).

The clustering of HN data yielded three regions (Fig. 4c): the first one (cluster 1) includes 52 stations having a median elevation of 603 m a.s.l. (min-max: 288-948 m a.s.l.), the second one (cluster 2) comprises 45 sites having a median altitude of 829 m a.s.l. (min-max: 625-1137 m a.s.l.), whereas the cluster 3 includes 23 sites, all located in the Central Apennines (except one, Montevergine Observatory, which is situated in the Southern sector), having a median elevation of 1210 m a.s.l. (min-max:
390 800-1750 m a.s.l.). This classification is clearly conditioned not only by altitude but also by local climatic and topographic factors, which may generate large difference in snowfall amount among stations located at similar altitudes. Most of stations belonging to cluster 4 are located in the proximity of Majella and Marsicani mountains, where the orographic forcing and low-level wind convergence lines are able to strongly enhance the snowfall precipitation.



3.1 Climatology for 1971-2000 period

395 Starting from the clustering results, we have built up a reference climatology for different snow seasons: early season (from
November to January), winter season (from December to February), late season (from February to April) and full season (from
November to April). This seasonal partition is similar to that generally adopted in previous studies (e.g. Matiu et al., 2021),
with some small adjustments depending on the climatic features of the study area and on the elevation range of the available
stations. Fig. 5 presents the climatology 1971-2000 for SCD parameter. More specifically, for each of the four seasons
400 previously introduced, the altitudinal distribution of the average SCD (expressed in number of days) is shown. Each point
represents one station and is color-coded according to the membership cluster (note that we follow the same color-coding
adopted in Fig. 4). In addition, on each panel the cluster-averaged values and the associated spatial standard deviation are also
reported. As it could be expected, there is a clear altitudinal gradient that grows as the elevation increases. In full season, the
SCD average rises by ≈ 9 days from cluster 1 (which presents a climatological value of $12.9 (\pm 3.8)$ days) to cluster 2 ($22.0 (\pm$
405 $3.0)$ days) and by ≈ 11 days from cluster 2 to cluster 3 ($33.4 (\pm 4.6)$ days), whereas the difference among cluster 3 and cluster
4 ($59.4 (\pm 12.1)$ days) is steeper (it is 26 days). The relationship between average SCD and elevation is efficiently modelled
by a power fit, as testified by the coefficient of determination (R^2), which ranges between 0.72 (early season) to 0.78 (late
season). Note that the power curve function obtained for a determined season is sketched on the corresponding panel as black
solid line, assuming that the average snow cover duration is the dependent variable (x) and the elevation the independent one
410 (y). It is interesting highlighting that the differences among clusters reduce in the early season, whereas they are larger in the
winter season. In addition, it is worth noting that in cluster 4 the distribution becomes more dispersed, as testified by the
standard deviation values. The spatial distribution of the average seasonal SCD over the study area is sketched in Fig. A1 in
Appendix A. In all seasons, the highest average SCD value has been found in Camposto (1430 m a.s.l.), which is located in a
plateau east of the Laga mountains. In this site, the local topographic conditions are particularly favourable to the persistence
415 of the snow on the ground.

The climatology for NDS is presented in Fig. 6. The average NDS values found for the available stations spread over the
considered altitudinal range following, also in this case, a distribution well captured by a power law function ($R^2 = 0.78$ for all
seasons). This behaviour suggests the existence of an altitudinal gradient, which, similarly to what has been discovered for
SCD, rises with increasing of elevation. The cluster-averaged climatological NDS values (shown for each season on the
420 corresponding panel) provide confirmation in this regards: in full season, the average NDS is $5.2 (\pm 0.7)$ days for cluster 1, 7.8
(± 1.3) days for cluster 2, $11.2 (\pm 1.9)$ days for cluster 3 and $20.0 (\pm 5.4)$ days for cluster 4. Above 800 m, there is a clear
increase of the spatial variability, which maximizes within cluster 4 in all seasons. The difference between clusters does not
exhibit a relevant seasonal dependence, although in winter a slight increment of the gap in average NDS value between cluster
1 and 2 and between cluster 3 and 4 has been detected. It is worth pointing out that, in full and late seasons, the highest
425 climatological NDS value has been observed in the Southern Apennines (Fig. A2), more precisely in Montevergine
Observatory (1280 m a.s.l.). This result is only apparently surprising. As briefly discussed in Section 2.1, the Southern



Apennines massifs included in the investigated area are well exposed to different air masses (i.e. to both continental air masses coming from Balkan regions and to maritime air masses coming from the Atlantic), so they receive larger precipitation amounts than the Central sectors. According to the results of our study, this aspect also reflects on the frequency of occurrence of snowfall events, which, on Partenio massif, is larger than many mountainous sites of the Central Apennines, located at the same altitude or slightly above, as demonstrated by Fig. A2.

The HN climatology is presented in Fig. 7. As for SCD and NDS, the analysed region exhibits a pronounced variability, mainly driven by the elevation, with a minimum, in the full season, of 24 cm in Lanciano (288 m a.s.l.) and a maximum of 335 cm in Monte Terminillo station (1750 m a.s.l.), in the Reatini Mountains. According to the scatter diagrams of Fig. 7, there is a clear separation between the three groups identified by the cluster analysis. In the full season, the climatological HN value is 44.5 (± 11.7) cm for cluster 1, 85.0 (± 18.5) cm for cluster 2 and 204.1 (± 51.9) cm for cluster 3. The latter shows a remarkable variability, which is related not only to the altitude but also to the incidence of orographic effects. In this respect, in the Abruzzo region there are several stations below 1000 m a.s.l. that received, in the considered reference period, relevant snowfall amounts, comparable to sites belonging to higher altitudinal bands. This is the case of Nerito (800 m a.s.l.), in which the full season climatological HN value is 148 cm, Rosello (890 m a.s.l.), in which the average HN value is 167 cm and Sant'Eufemia a Majella (870 m a.s.l.), the most impressive case, where the average HN value is 268 cm (Fig. A3). In the late and winter seasons, the snowfall amounts increase by $\approx 80\%$ from cluster 1 to cluster 2 and by $\approx 124\%$ from cluster 2 to cluster 3. In late season, we have detected a steeper altitudinal gradient, instead. The cluster 2 receives, on average, more than twice (+109.7%) the total HN value observed for cluster 1, whereas in cluster 3 the snowfall amounts grow by 150% with respect to cluster 2.

3.3 Trend analysis

The linear trend analysis has been applied to both individual SCD and NDS time series as well as to cluster-averaged time series. The latter have been obtained, for each of the investigated seasons, as the arithmetic mean of the values of stations belonging to a determined cluster.

Starting from SCD, Fig. 8 shows the cluster 1 (green solid line) and cluster 4 (blue solid line) time series for 1951-2001 period. Note that we decided not to plot the behaviour over time of cluster 2 and 3 only for ease of presentation. According to Section 3.1, cluster 1 and cluster 4 include stations belonging to different altitudinal bands (the median elevation is 648 and 1290 m a.s.l., respectively) and, therefore, they reflect two well-separated nivometric regimes. From a simple visual inspection of this figure, it clearly emerges that the investigated signals exhibit a negative tendency (see the black solid line). More specifically, the trend magnitude (expressed in number of days/10 years) is more pronounced in full season (-3.4 [-7.3 to 1.7] days/10 years for cluster 4 and -1.1 [-2.6 to 0.2] days/10 years for cluster 1) and in winter season (-3.2 [-6.0 to 0.0] days/10 years for cluster 4 and -1.1 [-2.5 to 0.2] days/10 years for cluster 1). Note that the values indicated in square brackets indicate the 95% confidence interval for linear trend. In the other seasons (early and late), the cluster 1 shows a negligible trend, whereas for cluster 4 a decreasing rate of -1.1 [-3.3 to 1.0] days/10 years and -1.8 [-4.5 to 0.6] days/10 years has been detected, respectively. As revealed by Table 3, the trends are statistically significant only in full and winter seasons. More specifically,



460 in winter season a negative tendency significant at 90% level has been found for clusters 1, 2 and 4, whereas for cluster 3 the
linear trend is significant at 95% confidence level. In full season, robust tendencies have been discovered only for cluster 1
and 4. According to Table 3, in all seasons the trend magnitude gradually increases from cluster 1 to cluster 4, so, in other
words, it rises with increasing altitude, especially in full and winter seasons. In addition, Table 3 shows, for each cluster, the
percentage of positive, negative and no trends (i.e. the aliquot of tendencies ranging between -0.4 and 0.4 days/10 years), and
465 the portion of trends significant at 95% confidence level. As can be expected, most of stations exhibit a negative tendency. In
particular, for clusters 2, 3 and 4, the percentage of negative trends is above 60% in all seasons and is greater than 90% for
clusters 3 and 4 in winter and for cluster 4 in full season. For cluster 1, there is a clear prevalence of negative trends only in
full and winter periods, whereas in early and late seasons most of the stations belonging to such cluster present a negligible
trend. Moreover, the fraction of significant and negative tendencies has an altitudinal dependency that is more linear and
470 evident in full and winter seasons. In the latter, half of the stations pertaining to cluster 3 and 4 exhibit a negative trend
significant at 95% confidence level. Another distinguishable behaviour of the signals sketched in Fig. 8 is the strong interannual
variability, which is particularly pronounced in cluster 4. This is a distinct feature of the precipitation records collected in mid-
latitudes that, with regard to Apennine area, has been just emphasized in previous works (Capozzi et al., 2022). Focusing on
full season, in cluster 4 the highest SCD values have been observed in 1962/63 season (105.3 days), 1952/53 (98.2 days) and
475 1980/81 (95.8 days), whereas the lowest SCD values have been observed in 1989/90 season (10.6 days), 2000-01 (22.0 days)
and 1963/64 (26.0 days). The season 1962/63 was notable in terms of SCD also for cluster 1 (43.0 days), although the highest
value for this group has been observed in 1955/56 (45.6 days), one of the coldest and snowiest seasons of the 20th century (e.g.
D'Errico et al., 2022). In cluster 1, the lowest values have been recorded in 1989/90 (0.9 days), 1960/61 (2.6 days) and in
1963-64 season (2.7 days). Superimposed to the decreasing trend, the Apennine's SCD also shows considerable decadal
480 variations, well captured by the 10-years locally weighted scatterplot smoothing (lowess). The latter, marked as red line in Fig.
8, is a robust non-parametric regression technique proposed by Cleveland (1979). By inspecting the behaviour of lowess fit, it
is possible to detect four periods characterized by extensive duration of snow cover, the early 1950s, the 1960-1970 period,
the late 1970s-early 1980s and the early 1990s, and four time segments with reduced SCD, the late 1950s, the mid-1970s, the
late 1980s and the late 1990s. The decadal oscillation of SCD seems to be a common features of all considered seasons and is
485 more relevant in cluster 4 time series.

The NDS time series exhibit a behaviour very similar to that described for SCD, as demonstrated by Fig. 9. For both clusters
1 and 4, we have detected a gradual decrease of the frequency of occurrence of snowfall events, again particularly pronounced
in full and winter seasons. In the former, the linear trend analysis revealed a negative tendency of -1.7 [-3.0 to -0.5] days/10
years for cluster 4 and of -0.8 [-1.3 to -0.1] days/10 years for cluster 1, whereas in the latter the tendency magnitude is -1.6
490 [-2.5 to -0.6] days/10 years for cluster 4 and -0.6 [-1.2 to -0.1] days/10 years for cluster 1. Such trends are statistically
significant at 95% confidence level, as indicated by Table 4. Strong negative tendencies have been also found, in full and
winter seasons, for the other cluster-averaged time series (except for cluster 2, whose trend is not statistically significant in full
season). As for SCD, in late season cluster-averaged trends are negligible and range between -0.1 [-0.7 to 0.4] days/10 years



(cluster 2) and -0.6 [-1.6 to 0.2] days/10 years (cluster 4). In the early season, negative trends significant at 90% level have
495 been detected for cluster 3 and 4 (trend magnitude is -0.6 [-1.2 to -0.1] days/10 years and -0.9 [-1.6 to -0.3] days/10 years,
respectively). Table 4 shows that long-term tendencies taking a direction towards NDS reduction are prevalent in all seasons
for cluster 3 and 4, with percentage up to 97-100% in winter season, whereas this result is not valid for cluster 1 and 2, in
which the no trend fraction predominates in the early and late seasons. The percentage of stations having a trend significant at
95% confidence level found for clusters 3 and 4 as well as the trend magnitude are substantially larger than that discovered for
500 clusters 1 and 2. Such results suggest the existence of a relationship between long-term tendency and elevation in terms of
statistical significance and magnitude. The decadal trend emerged from the analysis of SCD time series is also evident in NDS
signals, as highlighted by the lowess fit in Fig. 9. Similarly to what has been observed for SCD, this decadal behaviour is more
pronounced in cluster 4. The NDS signals also exhibited a very strong interannual variability, especially in the 1950-1960s. In
cluster 4, the frequency of occurrence of snowfall was particularly higher in 1962/63 full season (40.1 days), in 1955/56 (36.8
505 days) and in 1969/70 (33.0 days). It is interesting highlighting that the second and the third snow seasons more lacking in snow
events occurred in the 1950-1960s: the 1963-64 (7.7 days) and the 1958/59 (9.7 days). The lowest NDS value has been detected
in the 1989/90 season (5.1 days). The latter has been the weakest season in terms of snowfall occurrence also for cluster 1 (0.3
days). Very low values (1.6 and 1.4 days, respectively) have also been observed in 1963/64 and in 1960/61, respectively. The
1962/63 (21.5 days), the 1955/56 (18.1 days) and the 1953/54 (14.5 days) were the three richest seasons in terms of snow
510 episodes for cluster 1, instead.

Linear trends for individual stations as function of elevation at seasonal time scales are sketched in Fig. 10 (SCD) in Fig. 11
(NDS). Such diagrams provide more compelling evidence about the relationship between trend magnitude and altitude. As a
general result, a moderate correlation between the two variables has been found for both snow indicators. More specifically,
for SCD, the correlation is stronger in late and winter seasons ($\rho = |0.63|$ and $|0.62|$, respectively), whereas it is slightly weaker
515 in late season ($\rho = |0.43|$). For NDS, different results emerged in terms of seasonal variability of the correlation. The latter
maximizes in early season ($\rho = |0.59|$), whereas it is lower in late season ($\rho = |0.46|$). A visual comparison between Fig. 10 and
11 also reveals that SCD trends are characterized by a larger variability than NDS, especially at altitudes greater than 1000 m.
It is worth notice that in full season the maximum negative trend (-7.6 [-11.8 to -2.4] days/10 years) was found for Capracotta
(1400 m a.s.l.), a station belonging to cluster 4. The maximum positive tendency (1.4 [-3.7 to 6.0] days/10 years) has been
520 detected for Pietracamela (1000 m a.s.l.), a station that is part of the same cluster. This result well synthesizes the strong
variability and uncertainty that affect the linear trend estimation at high elevation ranges, which can be interpreted as a
consequence of the strong year-by-year fluctuations as well as of the local orographic effects incidence.



525 4 Discussions

4.1 Comparison with previous studies

In this study, thanks to the rescue of a large amount of manually snowfall observations collected by NHMS during the 1951-2001, it was possible to build-up a new, updated and solid reference climatology for an area, the Apennine regions, in which the information about past nivometric regime are scarce and very fragmented. For all considered snow indicators and for all investigated seasons, we found a relevant altitudinal gradient that grows as the elevation increases. This result exhibited a seasonal dependence for SCD and HN. More specifically, in the first case the altitudinal gradients are steeper in winter and reduce in the early season, whereas for HN the altitudinal gradient is more pronounced in late season. The clusters including the stations above 1000 m a.s.l. showed a strong spatial variability, mainly related to the orographic effects. In this respect, our results are in accordance with some previous works (e.g. Blanchet et al., 2009; Bertoldi et al., 2023), related to the Alpine region.

Our analysis has revealed that in the considered Apenninic region the SCD and NDS parameters exhibited a similar behaviour in terms of long-term and decadal trend. For both variables, a decreasing tendency has been detected in the 1951-2001 period. The observed variations are strongly connected with the season (i.e. they are more relevant in winter) and show a marked dependence from the elevation. It is obviously not straightforward contextualize such results in the available literature, because linear trends magnitude and their statistical significance are strongly dependent from the analysed time window. Focusing on papers that considered periods having a good overlap with the present work, it clearly emerge that our study confirms the local and general tendencies observed for SCD and NDS in the Mediterranean area. Regarding SCD, the declining tendency highlighted in this study is in agreement with the local trends found for Apennines (e.g. Petriccione and Bricca, 2019; Annella et al., 2023), as well as with the outcomes presented for several Alpine regions (e.g. Klein et al., 2016; Marcolini et al., 2017b; Marke et al., 2018; Matiu et al., 2021; Bertoldi et al., 2023). Another common point between our results and previous works lies in the elevation dependence of SCD trends. More specifically, this aspect has been discussed in Marcolini et al. (2017b), which analysed SCD and HS time series collected in the Adige catchment (North-East of Italy) from 1980 to 2009. They found a reduction in both variables at low and high altitude sites, although a difference emerged between the behaviour of stations located above and below 1650 m a.s.l.. In sites located below this altitude threshold, the decline in both SCD and HS was larger. This work concludes that areas under 1650 m a.s.l. are more sensitive to climate variability and to temperature increase than high elevation regions. Matiu et al. (2021) have reported a similar and more generalized result for the Alpine region: they found a decreasing trend in SCD below 2000 m a.s.l., while above no remarkable variations have been detected, at least in the period from November to May. The elevation dependence of snowfall trends has been also highlighted in a very recent work (Bertoldi et al., 2023) focused on the northeastern Italian Alps. Although this study is focused on HN indicator, it reported evidences comparable, at least in part, with SCD-based studies. On monthly basis, negative trends were found in the lowest elevation range (0-1000 m a.s.l.), some positive trends from January to March above 2000 m a.s.l., while the intermediate



elevation band (1000-2000 m a.s.l.) showed a strong variability with no robust tendencies. Averaged seasonal trends are negative for all elevation ranges, instead: in absolute terms, the maximum negative trend was found at intermediate levels. Unfortunately, the stations available in our study cover a limited altitudinal band (the only stations situated above 2000 m a.s.l., Campo Imperatore, has a very limited data availability), so we are not able to reconstruct the behaviour of SCD and NDS trends over the elevation range considered in previous studies for Alps and to identify a critical altitudinal band that separates different regimes characterized by opposite trend direction. Overall, the results of our study show that low and intermediate Apenninic levels (288-1430 m a.s.l.) are experiencing a decline in SCD that is similar to what generally observed in the Alps. However, in our case, most of the significant trends have been found in the core of the snow season (i.e. in the winter), whereas in the Alps the percentage of negative trends was substantially higher in spring months (e.g. Matiu et al., 2021). The NDS is a less-studied variable than other snow indicators, such as SCD, HN and HS. Our results confirm some evidence found in Switzerland by Marty (2008). From this study, in fact, a long-term downward tendency in snow days emerged for the 1948-2007 period. The decreasing NDS signal is stronger in the low altitude zone, whereas the higher stations showed a marked variability. Terzago et al. (2010) also found a decrease in NDS for the Piedmont region (1971-2009 period). In a subsequent work, related to a more extended period (1926-2010), Terzago et al. (2013) discovered a decline of the fraction of precipitation falling as snow for the Western Alps; in line with our study, the dropping in snow events was found to be more relevant in winter season.

As stated in the Section 1, ground observations are crucial for assessment of long-term snow variability and trends, especially in mountainous areas. However, it is necessary bear in mind that manual snowfall measurements have several limitations, mainly related to observer's errors in reading and recording the measurement and in poor siting (WMO, 2008). A possible source of uncertainty that affect the dataset rescued in this study, and consequently the results just discussed, is related to the incorrect counting of snow days in a determined month (i.e. NDS parameter). As an example, the observer might have considered as snowy, a day in which snowfall occurred without leaving any trace on the ground. In addition, in many contexts the HN measurements can be very doubtful due to the environmental conditions, such as turbulence and/or strong winds, which may generate snow drifts and spatial inhomogeneity in snow depth.

4.2 Connections with large-scale atmospheric patterns

A natural evolution of our study is a further investigation aimed to identify the main drivers controlling the SCD and NDS variability in the considered Apennines region. Recently, several research activities (e.g. Hammond et al., 2018; Annella et al., 2023; Bertoldi et al., 2023) dealt with this topic, taking into account both “local” variables, such as temperature and precipitation, as well as “global” drivers such as the large circulation patterns. According to the general results achieved for the Alpine region, the role of temperature and precipitation in controlling the snow presence is strongly modulated by the elevation. More specifically, at low elevations most of the snowfall variability is explained by temperature, whereas at high elevation the precipitation has a greater relative importance (e.g. Bertoldi et al., 2023). For the Apennines, Annella et al. (2023)



590 found that the reduction in SCD observed in Montevergine Observatory could be mainly attributed to the increasing trend in
temperature, which was statistically significant in winter and late seasons in the considered time interval (1931-2008). In light
of such results, it may be speculated that the decline in SCD and NDS discovered in our study has been mainly driven by the
rising temperature tendency occurred in the second half of XIX century. Currently, we are not able to demonstrate this
assumption with a deep investigation. Most of the historical temperature and precipitation records collected in the study area,
595 in fact, are not accessible into a ready-to-use digitized format. Therefore, a complete attribution analysis is left for future
analysis. However, here we discuss some preliminary linkages between the decadal trend observed in our study for SCD and
NDS signals and the large-scale circulation patterns. More specifically, our analysis starts from the results of Annella et al.
(2023). From this study, it emerged that short-time and decadal fluctuations of SCD in Montevergine Observatory are strongly
modulated by two teleconnections patterns, the Arctic oscillation (AO) and the Eastern Mediterranean Pattern (EMP). The first
600 one is a fundamental mode of the Northern Hemisphere climate variability as it describes simultaneous shift in several features
of the polar vortex (air temperature, air pressure and the location and strength of the jet stream). The EMP has been introduced
by Hatzaki et al. (2007) and is referred as the difference in 500-hPa geopotential height anomaly between the Eastern Atlantic
and the Eastern Mediterranean. Using the Wavelet tool, we search for relationship between these two large-scale patterns and
SCD and NDS signals. Note that the corresponding index for AO (the AO index, hereafter AOI) has been retrieved from
605 Climate Prediction Centre of the NOAA's National Weather Service (Climate Prediction Centre, 2024), whereas the EMP
index (hereafter, EMPI) was reconstructed in Capozzi et al. (2022) using the version 3 of the Twentieth Century Reanalysis
dataset (Allen et al., 2011), following the method described in Hatzaki et al. (2009). The XWT between AOI and SCD cluster-
averaged time series did not reveal noticeable results, except for winter season, in which a significant common power area on
2-year band has been detected between 1960 and 1965. In this region of the time-frequency spectrum, the AOI and SCD are
610 in anti-phase relationship. More interesting evidence came from the analysis of the relationship between EMP and SCD. Fig.
12 presents the XWT between EMPI and SCD cluster 4 time series for all four considered seasons. We have chosen the cluster
4 SCD time series as reference for this analysis because its behaviour in the time-frequency spectrum can be regarded as highly
representative of the one observed for other three clusters. This aspect has been confirmed by the CWT, which depicts a
coherent picture among the clusters, characterized by a significant peak in the ≈ 12 -14 year band from 1960s to 1990s and by
615 two high-frequency (≈ 2 year) oscillations, one located between 1951 and 1955 and the other one between 1960 and 1965. The
only exception is the cluster 1, in which the decadal oscillations are not statistically relevant. Starting from full season (Fig.
12a), it is easy to detect a significant common power in the ≈ 12 -16 year band from 1955 to 1985 and between 1960 and 1965
in the ≈ 0 -2 year band. A close connection between EMPI and SCD can be also found, on ≈ 12 -14 year band, in the early
season (Fig. 12b) from 1965 to 1985, whereas in winter (Fig. 12c) the common power area on decadal scale is restricted
620 between early 1960s and early 1970s and falls entirely within the cone of influence. A very strong and significant connection
between the investigated signals has been found in late season (Fig. 12d) on ≈ 12 -16 year band. The common power area, in
this case, extends from late 1950s to mid-1990s, so it embraces almost the entire analysed period. Some linkages in the high-
frequency region has been also detected between 1955 and 1965 (≈ 5 year), in 1985-1990 (≈ 0 -2 year band) in early season,



between late 1970s and early 1980s ($\approx 0-2$ year band) in winter season, and, finally, in the 1960-1965 and in the early 1970s
625 ($\approx 0-2$ year in both cases) in late season. The right pointing black arrows in the significant power areas indicate that EMPI and
SCD clearly swing in phase on decadal time scale, adding further evidence about the close time-frequency connection among
the signals. The XWT between EMPI and NDS cluster 4 time series draw a similar picture, as testified by Fig. 13. In this case,
there is a close and significant connection on decadal scale only in full season (Fig. 13a) and in late season (Fig. 13d). The
common power areas are localized in the same spectrum regions mentioned for SCD. In the $\approx 0-2$ year band, relevant
630 connections between EMPI and NDS have been found in 1961-1965 period in all seasons, between late 1970s and early 1980s
in winter (Fig. 13c) and in the early 1970s in late season. In early season (Fig. 13b), a common power area also appear in the
 ≈ 5 year band between mid-1950s and mid-1960s. The two signals are generally in a close in-phase relationship, except for
some significant areas in the high-frequency region, in which there is a slight lag between the two signals.

The direct in-phase connection existing between the investigated snow indicators and the EMPI is in line with what it should
635 be reasonably expect about the influence of EMP on snowfall variability in the Central and Southern Apennines. The positive
phase of EMP pattern, in fact, is associated with positive 500-hPa geopotential anomalies over northern Atlantic and with
negative ones over Central and Eastern Mediterranean basins (Hatzaki et al., 2007). This synoptic pattern generally drives
Arctic or Polar cold continental air masses towards Italy and, therefore, is clearly favourable to snowfall occurrence and
persistence on the ground in the Apennines, as previously demonstrated in Capozzi et al. (2022) and in Annella et al. (2023).
640 The negative phase of EMP depicts a very different configuration, which generally brings mild weather conditions in the
considered area.

It is interesting pointing out that the linkages between EMP and snow indicators has not been reported in any previous work
related to the Alpine region. For this area, most of the available studies searched for connections with other large-scale
circulation patterns, such as the North Atlantic Oscillation (NAO), the AO and the Mediterranean Oscillation. The results are
645 generally ambiguous and strongly dependent on the considered region and time interval (e.g. Durand et al., 2009, Kim et al.,
2013; Marcolini et al., 2017b; Bertoldi et al., 2023).

5 Conclusions

According to the Intergovernmental Panel on Climate Change (IPCC) report on high mountain (Hock et al., 2019), a general
decrease in snow cover duration, glaciers and permafrost due to climate change has occurred in last decades. The strong loss
650 in mountain cryosphere is likely to have relevant repercussions for global population who rely on the water stored in mountain
snow and ice for their water supply. Despite the serious impacts of mountain cryosphere loss, for several reasons many
mountain areas remain under-researched. In the Mediterranean, an example in this sense is represented by the Apennine region.
A considerable lack, in fact, exists in the knowledge of the past snowfall variability for this area, although it has a good heritage
of past in situ observations. This study has provided a contribution to bridge this gap, through the rescue and the analysis of
655 the snow precipitation measures manually collected between 1951 and 2001 by the Italian National Hydrological and



Mareographic Service in an area including a large part of the Central and Southern Apennines. After being subjected to quality check and homogenization procedures, the rescued dataset, consisting of monthly data of snow cover duration (SCD), number of days with snow (NDS) and height of new snow (HN), has been primarily analysed to retrieve a reference climatology (1971-2000 period). To pursue this aim, using a methodology based on Principal Component Analysis and k-means clustering, for
660 each snow indicator we have grouped the available stations in different clusters. This classification has been mainly driven by the altitude and, secondly, by other factors controlling the spatial variability of snow precipitation, such as the distance from sea, the site exposure, the hours of direct sunlight and local orographic features. The presented snowfall climatology greatly enhances and expands the existing historical database of several key snow-related variables, SCD, NDS and HN, for which continuous and high-quality measures are difficult to find. In addition, it constitutes an added value for researches focused on
665 the comprehension of climate dynamics in mountainous area as well as on future changes in snowfall in the Mediterranean Region and provides useful information for a wide range of application fields, concerning also the socio-economic impacts of snow precipitation.

Furthermore, using familiar statistical methodologies (the Sen's slope estimator and the Mann-Kendall test), we have identified the linear trend for SCD and NDS time series (the HN series have not considered for this analysis due to the limited length of
670 the available records). Both variables exhibited a negative tendency for the 1951-2001 period. We found that SCD and NDS trends are strongly dependent on altitude, in terms of magnitude and level of confidence. More specifically, the signal of decrease in length of snow cover on the ground and in the frequency of occurrence of snowfall gradually grows with the altitude and is generally very strong for stations located above 1000 m a.s.l.. Considering the entire snow season (i.e. the full season, from November to April), SCD trends statistically significant at 90% confidence level have been discovered for cluster
675 1 (-1.1 [-2.6 to 0.2] days/10 years) and for cluster 4 (-3.4 [-7.3 to 1.7] days/10 years). For NDS, trends significant at 95% confidence level have been detected for cluster 1, 3 and 4 (-0.8 [-1.3 to -0.1] days/10 years, -1.2 [-2.2 to -0.2] days/10 years and -1.7 [-3.0 to -0.5] days/10 years, respectively). At seasonal scale, the larger fraction of negative and significant trends has been found in winter season for both variables. In early and late seasons, the aliquot of significant tendencies strongly reduces, especially in clusters 1 and 2. In addition, we found that SCD trends exhibit a more pronounced variability and
680 uncertainty than NDS, especially in cluster 4 (which includes, for both snow indicators, only stations above 1000 m a.s.l.). In the considered Apenninic area, the SCD and NDS variables also show fluctuations at decadal scale as well as a remarkable interannual variability, in accordance with the findings of previous studies (e.g. Annella et al., 2023). The decadal behaviour gradually emerges with increasing altitude and is particularly relevant in cluster 4.

Despite some uncertainties and source of errors, which have been briefly discussed in the previous section, this study can be
685 considered the first wide-Apenninic assessment of snow climatology and long-term trend based on in situ observations. The information provided by this work add a contribution to the reconstruction of historically snowfall variability in the mountainous areas and pave the way for many future research activities. In this respect, future studies will be primarily devoted to deeply understand the physical mechanisms that control the evolution over time of the investigated snow variables. Regarding this aspect, we provided some preliminary results means of a Wavelet Analysis. More specifically, from the Cross



690 Wavelet Transform of Eastern Mediterranean Pattern Index (EMPI) and cluster 4 SCD and NDS time series, it emerged a significant common power in the ≈ 10 -16 year band. The two signals are phase locked, so we can conclude that on decadal scale the SCD and NDS behaviour in the investigated Apennines area mirrors the evolution of EMP.

In addition, other efforts may be addressed to (i) extend back and forward the investigated period, in order to further increase the robustness of trend analysis and to contextualize the observed SCD and NDS tendencies in a broader time horizon and (ii)
695 to replicate this study for the northern Apennine sector and for the remaining sector of the Southern Apennine through the rescue of nivometric stations belonging to the other Italian National Hydrographic and Mareographic Service compartments.

Appendix A

700

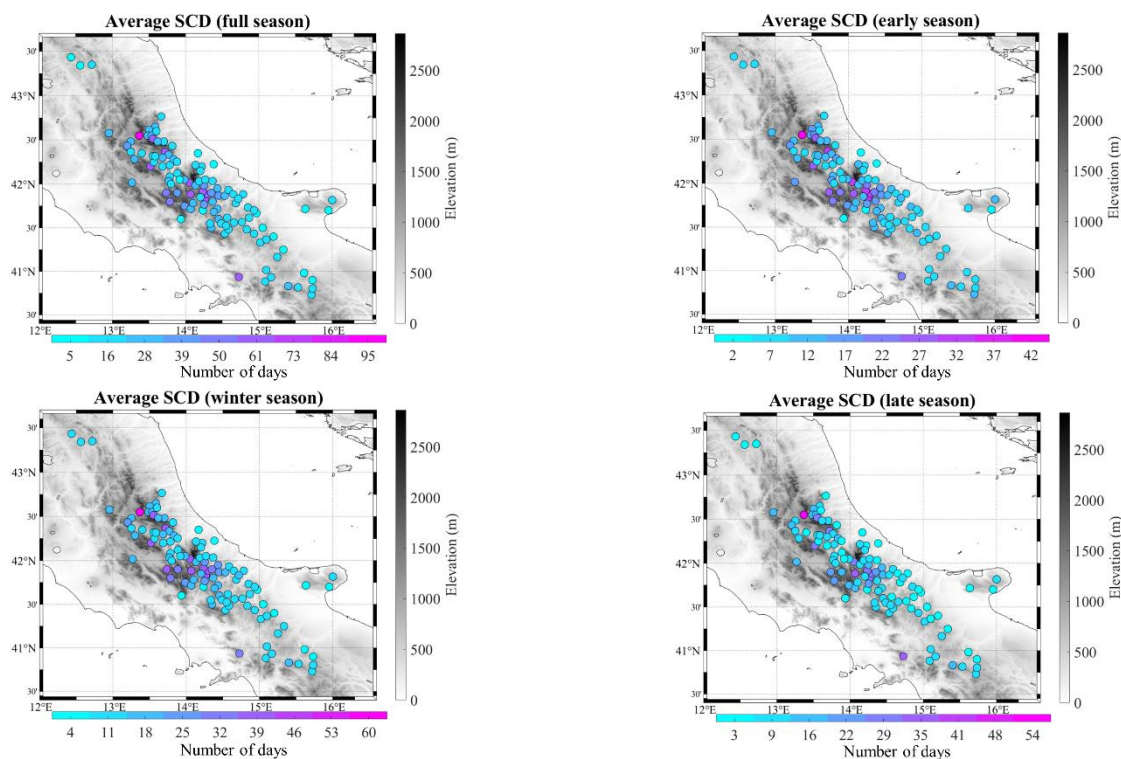
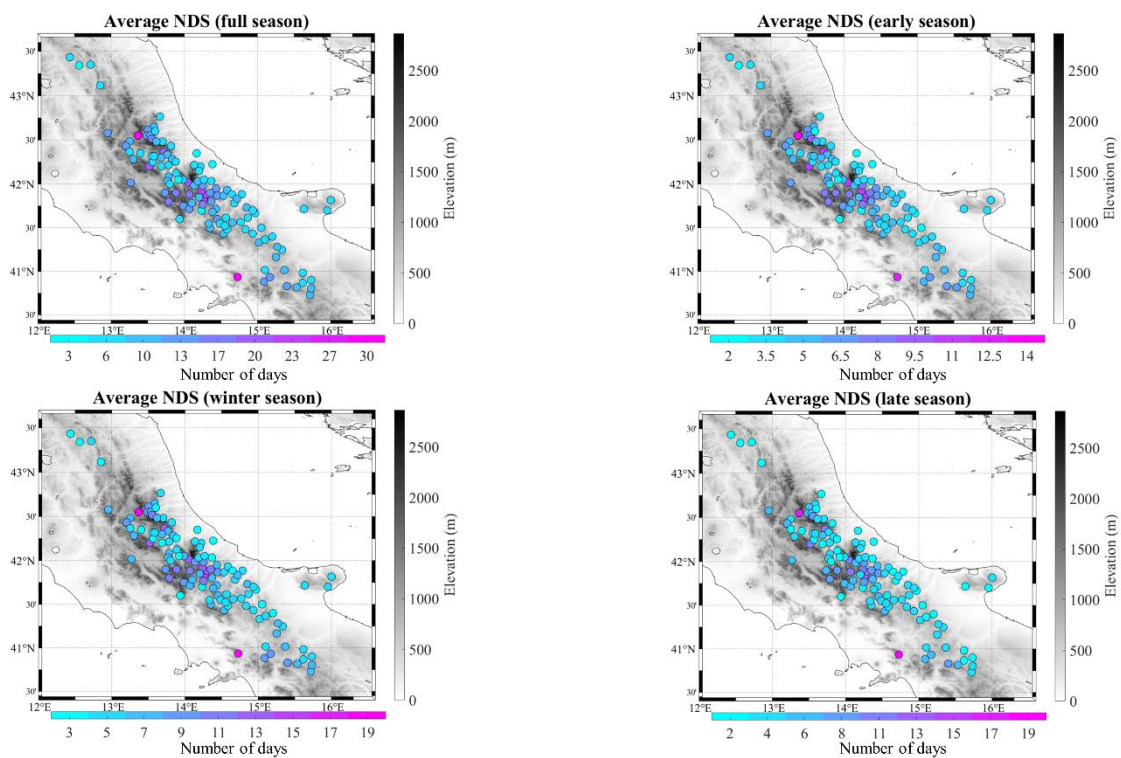


Figure A1: Spatial distribution of the average seasonal snow cover duration (SCD) over the study area in the period 1971-2000. Each point represents one station and the corresponding climatological value.

705



710 **Figure A2: Spatial distribution of the average seasonal number of days with snow (NDS) over the study area in the period 1971-2000. Each point represents one station and the corresponding climatological value.**

715

720

725

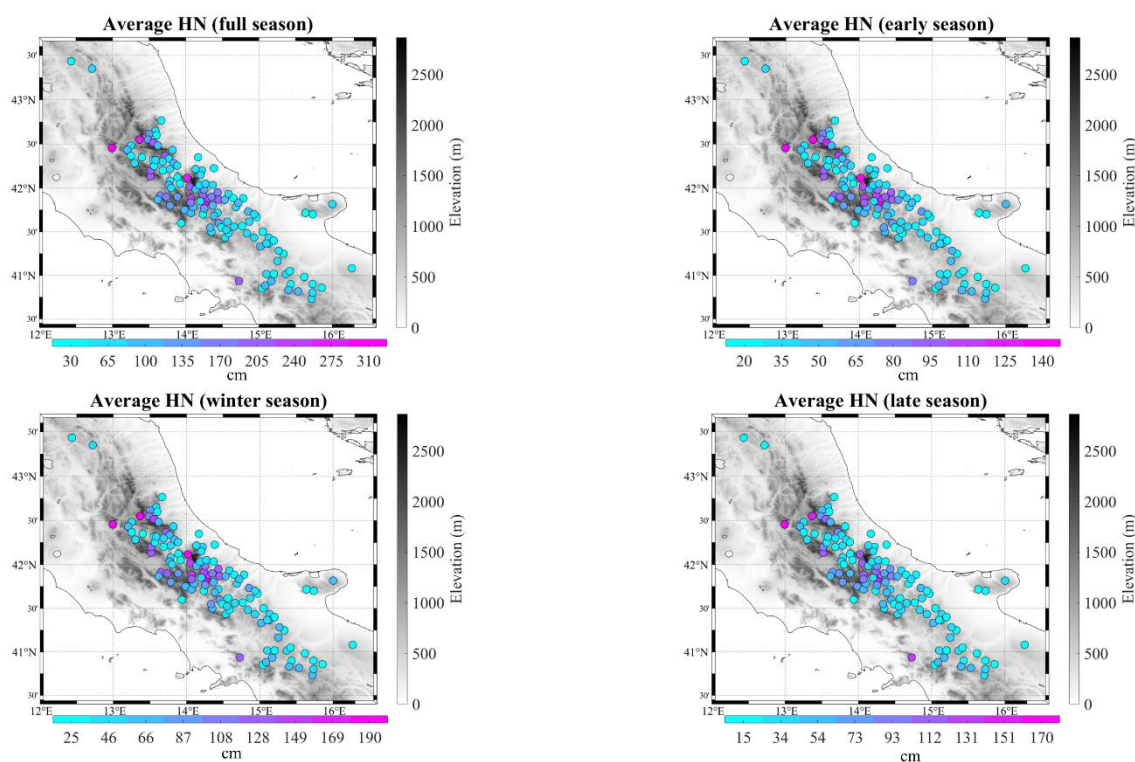


Figure A3: Spatial distribution of the average seasonal total height of new snow (HN) over the study area in the period 1971-2000. Each point represents one station and the corresponding climatological value.

730

735

Code/Data Availability: The data that support the findings of this study are available from the corresponding author, upon reasonable request.

Competing interests. The authors declare that they have no conflict of interests.

Author contribution: Conceptualization, V.C.; Data curation, F.S., A.R. and V.C.; Methodology, V.C. and C.A.; Formal analysis, V.C. and F.S.; Investigation, V.C. and C.A.; Writing—original draft preparation, V.C.; Writing—review and editing, C.A., A.R. and G.B.; Supervision, G.B. All authors have read and agreed to the published version of the manuscript.

740



References

- 745 Alexandersson, H.: A homogeneity test applied to precipitation data, *J. Climatol.*, 6, 661–675, 1986.
- Anderberg, M. R.: Cluster analysis for applications. New York: Academic Press, 1973.
- Annella, C., Budillon, G., and Capozzi, V.: On the role of local and large-scale atmospheric variability in snow cover duration: a case study of Montevergine Observatory (Southern Italy), *Environ. Res. Commun.*, 5, 031005, [10.1088/2515-7620/acc3e3](https://doi.org/10.1088/2515-7620/acc3e3), 2023.
- 750 Bartolini, E., Claps, P., and D'Odorico, P.: Connecting European snow cover variability with large scale atmospheric patterns. *Advances in Geosciences*, 26, 93–97, <https://doi.org/10.5194/adgeo-26-93-2010>, 2010.
- 755 Bartolomeu, S., Carvalho, M.J., Marta-Almeida, M., Melo-Gonçalves, P., and Rocha, A.: Recent trends of extreme precipitation indices in the Iberian Peninsula using observations and WRF model results, *Physics and Chemistry of the Earth, Parts A/B/C*, 94, 10–21, <https://doi.org/10.1016/j.pce.2016.06.005>, 2016.
- 760 Beaumet, J., Ménégoz, M., Morin, S., Gallée, H., Fettweis, X., Six, D., Vincent, C., Wilhelm, B., and Anquetin, S.: Twentieth century temperature and snow cover changes in the French Alps, *Regional Environmental Change*, 21(4), 114. <https://doi.org/10.1007/s10113-021-01830-x>, 2021.
- 765 Bertoldi, G., Bozzoli, M., Crespi, A., Matiu, M., Giovannini, L., Zardi, D., and Majone, B.: Diverging snowfall trends across months and elevation in the northeastern Italian Alps, *International Journal of Climatology*, 43(6), 2794–2819. <https://doi.org/10.1002/joc.8002>, 2023.
- Blanchet, J., Marty, C., and Lehning, M.: Extreme value statistics of snowfall in the Swiss Alpine region, *Water Resources Research*, 45(5), W05424, <https://doi.org/10.1029/2009WR007916>, 2009.
- 770 Bormann, K.J., Brown, R.D., Derksen, C., and Painter, T.H.: Estimating snow-cover trends from space, *Nat. Clim. Change*, 8, 924–8, <https://doi.org/10.1038/s41558-018-0318-3>, 2018.
- 775 Brönnimann, S., Annis, J., Dann, W., Ewen, T., Grant, A. N., Griesser, T., Krähenmann, S., Mohr, C., Scherer, M., and Vogler, C.: A guide for digitising manuscript climate data, *Clim. Past*, 2, 137–144, <https://doi.org/10.5194/cp-2-137-2006>, 2006.



- Brunetti, M., Maugeri, M., Nanni, T., Simolo, C., and Spinoni, J.: High-resolution temperature climatology for Italy: interpolation method intercomparison, *Int. J. Climatol.*, 34, 1278–1296, <https://doi.org/10.1002/joc.3764>, 2014.
- 780 Buchmann, M., Coll, J., Aschauer, J., Begert, M., Brönnimann, S., Chimani, B., Resch, G., Schöner, W., and Marty, C.: Homogeneity assessment of Swiss snow depth series: comparison of break detection capabilities of (semi-)automatic homogenization methods, *The Cryosphere*, 16, 2147–2161, <https://doi.org/10.5194/tc-16-2147-2022>, 2022.
- Buchmann, M., Resch, G., Begert, M., Brönnimann, S., Chimani, B., Schöner, W., and Marty, C.: The benefits of
785 homogenising snow depth series – Impacts on decadal trends and extremes for Switzerland, *The Cryosphere*, 17, 653–671, <https://doi.org/10.5194/tc-17-653-2023>, 2023.
- Caloiero, T., Coscarelli, R., Ferrari, E., and Mancini, M.: Trend detection of annual and seasonal rainfall in Calabria (southern Italy), *International Journal of Climatology*, 31(1), 44–56, <https://doi.org/10.1002/joc.2055>, 2011.
- 790 Capozzi, V., Cotroneo, Y., Castagno, P., De Vivo, C., and Budillon, G.: Rescue and quality control of sub-daily meteorological data collected at Montevergine Observatory (Southern Apennines), 1884–1963, *Earth Syst. Sci. Data*, 12, 1467–1487, <https://doi.org/10.5194/essd-12-1467-2020>, 2020.
- 795 Capozzi, V., De Vivo, C., and Budillon, G.: Synoptic control over winter snowfall variability observed in a remote site of Apennine Mountains (Italy), 1884–2015, *The Cryosphere*, 16, 1741–1763, <https://doi.org/10.5194/tc-16-1741-2022>, 2022.
- Capozzi, V., Annella, C., and Budillon, G.: Classification of daily heavy precipitation patterns and associated synoptic types in the Campania Region (southern Italy), *Atmospheric Research*, 289, <https://doi.org/10.1016/j.atmosres.2023.106781>, 2023.
- 800 Carey, S. K., Tetzlaff, D., Buttle, J., Laudon, H., McDonnell, J., McGuire, K., Seibert, J., Soulsby, C., and Shanley, J.: Use of color maps and wavelet coherence to discern seasonal and interannual climate influences on streamflow variability in northern catchments, *Water Resour. Res.*, 49, 6194–6207, doi:10.1002/wrcr.20469, 2013.
- 805 Cleveland, W.S.: Robust locally weighted regression and smoothing scatter plots, *Journal of the American Statistical Association*, 74(368), 829–836, <https://doi.org/10.1080/01621459.1979.10481038>, 1979.
- Climate Prediction Center: Climate Prediction Center: Northern Hemisphere Teleconnections Patterns, <https://www.cpc.ncep.noaa.gov/data/teledoc/telecontents.shtml>, last access: 10 January 2024.



810

Crespi, A., Brunetti, M., Lentini, G., and Maugeri, M.: 1961–1990 high-resolution monthly precipitation climatologies for Italy, *Int. J. Climatol.*, 38, 878–895, <https://doi.org/10.1002/joc.5217>, 2018.

815 Curci, G., Guijarro, J.A., Di Antonio, L., Di Bacco, M., Di Lena, B., Scorzini, A.R.: Building a local climate reference dataset: Application to the Abruzzo region (Central Italy), 1930–2019, *Int. J. Climatol.*, 41: 4414–4436, <https://doi.org/10.1002/joc.7081>, 2021.

820 D'Errico, M., Pons, F., Yiou, P., Tao, S., Nardini, C., Lunkeit, F., and Faranda, D.: Present and future synoptic circulation patterns associated with cold and snowy spells over Italy, *Earth Syst. Dynam.*, 13, 961–992, <https://doi.org/10.5194/esd-13-961-2022>, 2022.

De Bellis, A., Pavan, V., and Levizzani, V.: Climatologia e variabilità interannuale della neve sull'Appennino Emiliano Romagnolo, *Quaderno Tecnico ARPA-SIMC n°19/2010*, 118, 10.13140/2.1.4685.7287, 2010.

825 Diodato, N., Ljungqvist, F.C., and Bellocchi, G.: Empirical modelling of snow cover duration patterns in complex terrains of Italy, *Theor. Appl. Climatol.*, 147, 1195–212, <https://doi.org/10.1007/s00704-021-03867-8>, 2022.

830 Durand, Y., Giraud, G., Laternser, M., Etchevers, P., Mérindol, L., and Lesaffre, B.: Reanalysis of 47 Years of Climate in the French Alps (1958–2005): Climatology and Trends for Snow Cover, *J. Appl. Meteorol. Clim.*, 48, 2487–2512, <https://doi.org/10.1175/2009JAMC1810.1>, 2009.

Easterling, D. R. and Peterson, T.C.: A new method for detecting and adjusting for undocumented discontinuities in climatological time series, *International Journal Climatol.*, 15, 369–377, <https://doi.org/10.1002/joc.3370150403>, 1995.

835 Fazzini, M., Magagnini, L., Giuffrida, A., Frustaci, G., Di Lisciando, M., and Gaddo, M.: Nevosità in Italia negli ultimi 20 anni, *Neve e Valanghe*, 58, pp. 22-33, available online at <https://aineva.it/wp-content/uploads/Pubblicazioni/Rivista58/NV58.pdf> (last access on 05 February 2024), 2006.

840 Fazzini, M.: Caratterizzazione generale dei fenomeni di innevamento nel territorio italiano, *Neve e Valanghe*, 60, pp. 36-49, available online at: <https://aineva.it/wp-content/uploads/Pubblicazioni/Rivista60/NV60.pdf> (last access on 04 February 2024), 2007.



- 845 Fragoso, M. and Tildes Gomes, P.: Classification of daily abundant rainfall patterns and associated large-scale atmospheric circulation types in Southern Portugal, *Int. J. Climatol.*, 28: 537-544, <https://doi.org/10.1002/joc.1564>, 2008.
- Fugazza, D., Manara, V., Senese, A., Diolaiuti, G., and Maugeri, M.: Snow cover variability in the Greater Alpine region in the MODIS era (2000–2019), *Remote Sensing*, 13(15), 2945, <https://doi.org/10.3390/rs13152945>, 2021.
- 850 Gazzolo, T., and Pinna, M.: *La nevosità in Italia nel Quarantennio 1921- 1960 (gelo, neve e manto nevoso)*, Ministero dei Lavori Pubblici, Consiglio Superiore, Servizio Idrografico, Pubblicazione n. 26 del Servizio, Istituto Poligrafico dello Stato, Roma, 216 pp., 1973.
- Grinsted, A., Moore, J. C., and Jevrejeva, S.: Application of the cross wavelet transform and wavelet coherence to geophysical time series, *Nonlin. Processes Geophys.*, 11, 561–566, doi:10.5194/npg-11-561-2004, 2004.
- 855 Guijarro, J. A.: Homogenization of climatic series with Climatol, *Climatol manual*, https://www.climatol.eu/homog_climatol-en.pdf (last access: 15 February 2024), 2018.
- Hamed, K.H.: Trend detection in hydrologic data: the Mann–Kendall trend test under the scaling hypothesis, *Journal of Hydrology*, 349(3-4), 350–363, <https://doi.org/10.1016/j.jhydrol.2007.11.009>, 2008.
- 860 Hammond, J.C., Saavedra, F.A., and Kampf, S.K.: Global snow zone maps and trends in snow persistence 2001–2016, *International Journal of Climatology*, 38(12), <https://doi.org/10.1002/joc.5674>, 4369–4383, 2018.
- 865 Hatzaki, M., Flocas, H. A., Asimakopoulos, D. N., and Maheras, P.: The eastern Mediterranean teleconnection pattern: identification and definition. *Int. J. Climatol.*, 27, 727–737, <https://doi.org/10.1002/joc.1429>, 2007.
- Hatzaki, M., Flocas, H. A., Giannakopoulos, C., and Maheras P.: The impact of the eastern Mediterranean teleconnection pattern on the Mediterranean climate, *J. Climate*, 22, 977–992, <https://doi.org/10.1175/2008JCLI2519.1>, 2009.
- 870 Hock, R., Rasul, G., Adler, C., Cáceres, B., Gruber, S., Hirabayashi, Y., Jackson, M., Kääb, A., Kang, S., Kutuzov, S., Milner, A., Molau, U., Morin, S., Orlove, B., and Steltzer, H.: High Mountain Areas. In: *IPCC Special Report on the Ocean and Cryosphere in a Changing Climate* [H.-O. Pörtner, D.C. Roberts, V. Masson-Delmotte, P. Zhai, M. Tignor, E. Poloczanska, K. Mintenbeck, A. Alegría, M. Nicolai, A. Okem, J. Petzold, B. Rama, N.M. Weyer (eds.)], 2019.
- 875



Italian Institute for Environmental Protection and Research (ISPRA): Annali Idrologici Storici, <http://www.bio.isprambiente.it/annalipdf/>, last access: 09 January 2024.

880 Italian Institute for Environmental Protection and Research (ISPRA): Hydrological Yearbooks, <https://www.isprambiente.gov.it/en/projects/inland-waters-and-marine-waters/hydrological-yearbooks>, last access: 09 January 2024.

Kendall, M.G.: Rank correlation methods, 3rd edition. New York: Hafner Publishing Company, 1962.

885 Kidson, J.W.: An automated procedure for the identification of synoptic types applied to the new zealand region, *Int. J. Climatol.*, 14: 711–721, <https://doi.org/10.1002/joc.3370140702>, 1994.

Kim, Y., Kim, K.-Y., and Kim, B.-M.: Physical mechanisms of European winter snow cover variability and its relationship to the NAO, *Climate Dynamics*, 40(7), 1657–1669, <https://doi.org/10.1007/s00382-012-1365-5>, 2013.

890

Klein, G., Vitasse, Y., Rixen, C., Marty, C., and Rebetez, M.: Shorter snow cover duration since 1970 in the Swiss Alps due to earlier snowmelt more than to later snow onset, *Climatic Change*, 139, 637–649, <https://doi.org/10.1007/s10584-016-1806-y>, 2016.

895 Kotlarski, S., Gobiet, A., Morin, S., Olefs, M., Rajczak, J., and Samacoïts, R.: 21st century alpine climate change, *Climate Dynamics*, 60, 65–86, <https://doi.org/10.1007/s00382-022-06303-3>, 2022.

Kuya, E. K., Gjeltén, H. M., and Tveito, O. E.: Homogenization of Norwegian monthly precipitation series for the period 1961–2018, *Adv. Sci. Res.*, 19, 73–80, <https://doi.org/10.5194/asr-19-73-2022>, 2022.

900

Leporati, E. and Mercalli, L.: Snowfall series of Turin, 1784–1992: climatological analysis and action on structures, *Annals of Glaciology*, 19, 77–84, doi:10.3189/S0260305500011010, 1994.

905 Magnani, A., Viglietti, D., Godone, D., Williams, M.W., Balestrini, R., and Freppaz, M.: Interannual variability of soil N and C forms in response to snow-cover duration and pedoclimatic conditions in alpine tundra, northwest Italy, *Arctic, Antarctic, and Alpine Research*, 49, 227–42, <https://doi.org/10.1657/AAAR0016-037>, 2017.

Mann, H.B.: Nonparametric tests against trend, *Econometrica*, 13, 245–259, 1945.



910 Marcolini, G., Bellin, A., Disse, M., and Chiogna, G.: Variability in snow depth time series in the Adige catchment, *J. Hydrol. Reg. Stud.*, 13, 240–254, <https://doi.org/10.1016/j.ejrh.2017.08.007>, 2017b.

Marke, T., Hanzer, F., Olefs, M. and Strasser, U.: Simulation of past changes in the Austrian snow cover 1948–2009, *Journal of Hydrometeorology*, 19(10), 1529–1545, <https://doi.org/10.1175/JHM-D-17-0245.1>, 2018.

915

Marty, C.: Regime shift of snow days in Switzerland, *Geophysical Research Letters*, 35(12), L12501. <https://doi.org/10.1029/2008gl033998>, 2008.

Marty, C. and Blanchet, J.: Long-term changes in annual maximum snow depth and snowfall in Switzerland based on extreme
920 value statistics, *Climatic Change*, 111, 705–721, <https://doi.org/10.1007/s10584-011-0159-9>, 2012.

Matiu, M., Crespi, A., Bertoldi, G., Carmagnola, C. M., Marty, C., Morin, S., Schöner, W., Cat Berro, D., Chiogna, G., De
Gregorio, L., Kotlarski, S., Majone, B., Resch, G., Terzago, S., Valt, M., Beozzo, W., Cianfarra, P., Gouttevin, I., Marcolini,
G., Notarnicola, C., Petitta, M., Scherrer, S. C., Strasser, U., Winkler, M., Zebisch, M., Cicogna, A., Cremonini, R., Debernardi,
925 A., Faletto, M., Gaddo, M., Giovannini, L., Mercalli, L., Soubeyroux, J.-M., Sušnik, A., Trenti, A., Urbani, S., and Weilguni,
V.: Observed snow depth trends in the European Alps: 1971 to 2019, *The Cryosphere*, 15, 1343–1382,
<https://doi.org/10.5194/tc-15-1343-2021>, 2021.

Meteomont: Historical archive of weather and snow data, [https://meteomont.carabinieri.it/archivio-condizioni-](https://meteomont.carabinieri.it/archivio-condizioni-meteorologiche?lang=en)
930 [meteorologiche?lang=en](https://meteomont.carabinieri.it/archivio-condizioni-meteorologiche?lang=en), last access: 04/01/2024.

Meteomont: Manual weather stations data, <https://meteomont.carabinieri.it/stazioni-manuali?lang=en>, last access: 04 January
2024.

935 Mote, P.W., Li, S., Lettenmaier, D.P., Xiao, M., and Engel, R.: Dramatic declines in snowpack in the western US, *npj Climate and Atmospheric Science*, 1(1), 1–6, <https://doi.org/10.1038/s41612-018-0012-1>, 2018.

Notarnicola, C.: Hotspots of snow cover changes in global mountain regions over 2000–2018, *Remote Sensing of Environment*, 243, 111781, <https://doi.org/10.1016/j.rse.2020.111781>, 2020.

940

Olefs, M., Koch, R., Schöner, W., and Marke, T.: Changes in snow depth, snow cover duration, and potential snowmaking
conditions in Austria, 1961–2020—a model based approach, *Atmosphere*, 11(1), 7600,
<https://doi.org/10.3390/atmos11121330>, 2020.



945 Ortiz-Gómez, R., Muro-Hernández, L.J., and Flowers-Cano, R.S.: Assessment of extreme precipitation through climate change indices in Zacatecas, Mexico, *Theoretical and Applied Climatology*, 141, 1541–1557, <https://doi.org/10.1007/s00704-020-03293-2>, 2020.

Percival, D.B.: Analysis of Geophysical Time Series Using Discrete Wavelet Transforms: An Overview. In: Donner, R.V.,
950 Barbosa, S.M. (eds) *Nonlinear Time Series Analysis in the Geosciences*. Lecture Notes in Earth Sciences, vol 112, Springer, Berlin, Heidelberg, https://doi.org/10.1007/978-3-540-78938-3_4, 2008.

Petriccione, B. and Bricca, A.: Thirty years of ecological research at the Gran Sasso d'Italia LTER site: climate change in action, *Nature Conservation*, 34, 9–39, <https://doi.org/10.3897/natureconservation.34.30218>, 2019.

955

Scherrer, S. C., Wüthrich, C., Croci-Maspoli, M., Weingartner, R., and Appenzeller, C.: Snow variability in the Swiss Alps 1864–2009, *Int. J. Climatol.*, 33, 3162–3173, <https://doi.org/10.1002/joc.3653>, 2013.

Sen, P.K.: Estimates of the regression coefficient based on Ken-dall's tau, *Journal of the American Statistical Association*,
960 63(324), 1379–1389, <https://doi.org/10.2307/2285891>, 1968.

Song, X., Song, S., Sun, W., Mu, X., Wang, S., Li, J. et al.: Recent changes in extreme precipitation and drought over the Songhua River Basin, China, during 1960–2013, *Atmospheric Research*, 157, 137–152, <https://doi.org/10.1016/j.atmosres.2015.01.022>, 2015.

965

Sumner, G., Guijarro, J.A., and Ramis, C.: The impact of surface circulation on significant daily rainfall patterns over Mallorca, *Int. J. Climatol.*, 15: 673-696, <https://doi.org/10.1002/joc.3370150607>, 1995.

Tecilla, G.: L'indagine nazionale su neve e valanghe. Lo stato delle reti di monitoraggio e delle banche di dati nivometeorologici in Italia, *Neve e Valanghe*, 60, pp. 12-35, available online at <https://aineva.it/wp-content/uploads/Pubblicazioni/Rivista60/NV60.pdf> (last access on 06 February 2024), 2007.

Terzago, S., Cassardo, C., Cremonini, R., and Fratianni, S.: Snow Precipitation and Snow Cover Climatic Variability for the Period 1971–2009 in the Southwestern Italian Alps: The 2008–2009 Snow Season Case Study, *Water*, 2, 773–787,
975 <https://doi.org/10.3390/w2040773>, 2010.



- Terzago, S., Fratianni, S., and Cremonini, R.: Winter precipitation in Western Italian Alps (1926–2010), *Meteorol. Atmos. Phys.*, 119, 125–136, <https://doi.org/10.1007/s00703-012-0231-7>, 2013.
- 980 Torrence, C. and Compo, G. P.: A practical guide to wavelet analysis, *Bull. Am. Meteorol. Soc.*, 79, 61–78, [https://doi.org/10.1175/1520-0477\(1998\)079<0061:APGTWA>2.0.CO;2](https://doi.org/10.1175/1520-0477(1998)079<0061:APGTWA>2.0.CO;2), 1998.
- Tramblay, Y., El Adlouni, S., and Servat, E.: Trends and variability in extreme precipitation indices over Maghreb countries, *Nat. Hazards Earth Syst. Sci.*, 13, 3235–3248, <https://doi.org/10.5194/nhess-13-3235-2013>, 2013.
- 985 Valt, M. and Cianfarra, P.: Recent snow cover variability in the Italian Alps, *Cold Reg. Sci. Technol.*, 64, 146–157, <https://doi.org/10.1016/j.coldregions.2010.08.008>, 2010.
- Vernay, M., Lafaysse, M., Monteiro, D., Hagenmuller, P., Nheili, R., Samacoïts, R., Verfaillie, D., and Morin, S.: The S2M meteorological and snow cover reanalysis over the French mountainous areas: description and evaluation (1958–2021), *Earth System Science Data*, 14(4), 1707–1733, <https://doi.org/10.5194/essd-14-1707-2022>, 2022.
- 990 World Meteorological Organization: Guide to Meteorological Instruments and Methods of Observation, 2008 Edition, WMO-no. 8 (Seventh edition), available at: https://www.wmo.int/pages/prog/www/IMOP/publications/CIMO-Guide/OLD-pages/CIMO_Guide-7th_Edition-2008.html (last access: 01 February 2024), 2008.
- 995 World Meteorological Organization: Guidelines on Best Practices for Climate Data Rescue 2016, WMO-No. 1182, available at: <https://public.wmo.int/en/resources/library/guidelines-best-practices-climate-data-rescue> (last access: 15 January 2024), 2016.

1000

1005

1010



LIST OF TABLES

Table 1. Main settings used to run Climatol (Guijarro, 2018) for quality control and homogenization of the investigated SCD, NDS and HN time series.

Parameter	SCD	NDS	HN	Description
std	1	1	2	Type of data normalization: 1 = deviation from the mean; 2 = ratios to the mean
wz	0.1	0.1	0.1	Scale parameter of the vertical coordinate
dz.max	15	15	20	Threshold of outlier tolerance, in standard deviations
snht1	25	32	30	Detection thresholds of changes in the mean of the series
snht2	40	40	40	(determined by the explanatory analysis)

1015

Table 2. For each of the investigated snow indicators (SCD, NDS and HN), the number of stations belonging to a determined cluster and the stations' median and range elevation (minimum-maximum) are shown.

Cluster	Number of stations			Elevation (m a.s.l.)		
	SCD	NDS	HN	SCD	NDS	HN
1	58	31	52	648 (288-910)	569 (288-850)	603 (288-948)
2	26	34	45	815 (550-954)	700 (520-910)	829 (625-1137)
3	14	35	23	1000 (750-1157)	879 (650-1375)	1210 (800-1750)
4	12	14	/	1290 (1000-1430)	1220 (1000-1430)	/

1025



1030 **Table 3.** For each cluster (CL) and for each season (full (F), early (E), winter (W) and late (L)), the average SCD trend value (expressed as number of days per 10 years), the percentage of positive and negative trend and the percentage of no trend are presented. For both positive and negative trend, the fraction of significant tendencies is also indicated. Note that no trend are defined as tendencies ranging between -0.4 and 0.4 days/10 years. The trend confidence level is coded as follows: **for 95%, * for 90%.

CL	Average SCD trend (days/10 years)				Positive trends (%)				Negative trends (%)				No trend (%)											
	F	E	W	L	Tot.		Sig.		Tot.		Sig.		F		E		W		L					
					F	E	W	L	F	E	W	L	F	E	W	L	F	E	W	L				
1	-1.1*	-0.4	-1.1*	-0.3	3	2	0	0	0	0	0	0	72	43	81	28	21	14	24	7	24	55	19	72
2	-1.3	-0.6	-1.7*	-0.3	8	8	0	8	0	0	0	0	73	73	86	62	27	12	35	4	19	19	12	31
3	-3.0	-1.1	-2.8**	-1.4	0	7	0	0	0	0	0	0	86	86	93	86	36	36	50	7	14	7	7	14
4	-3.4*	-1.1	-3.2*	-1.8	8	17	0	8	0	0	0	0	92	67	92	83	42	17	50	42	0	17	8	8

1035

Table 4. For each cluster (CL) and for each season (full (F), early (E), winter (W) and late (L)), the average NDS trend value (expressed as number of days per 10 years), the percentage of positive and negative trend and the percentage of no trend are presented. For both positive and negative trend, the fraction of significant tendencies is also indicated. Note that no trend are defined as tendencies ranging between -0.4 and 0.4 days/10 year. The trend confidence level is coded as follows: **for 95%, * for 90%.

CL	Average NDS trend (days/10 years)				Positive trends (%)				Negative trends (%)				No trend (%)											
	F	E	W	L	Tot.		Sig.		Tot.		Sig.		F		E		W		L					
					F	E	W	L	F	E	W	L	F	E	W	L	F	E	W	L				
1	-0.8**	-0.3	-0.6**	-0.3	0	0	0	0	0	0	0	0	71	32	71	13	48	29	52	0	29	68	29	87
2	-0.6	-0.3	-0.7**	-0.1	0	0	0	0	0	0	0	0	65	32	79	14	32	24	29	3	35	68	21	85
3	-1.2**	-0.6*	-1.2**	-0.5	0	0	0	0	0	0	0	0	89	83	97	60	60	46	69	29	11	17	3	40
4	-1.7**	-0.9*	-1.6**	-0.6	0	0	0	0	0	0	0	0	93	86	100	79	71	71	79	14	7	14	0	21

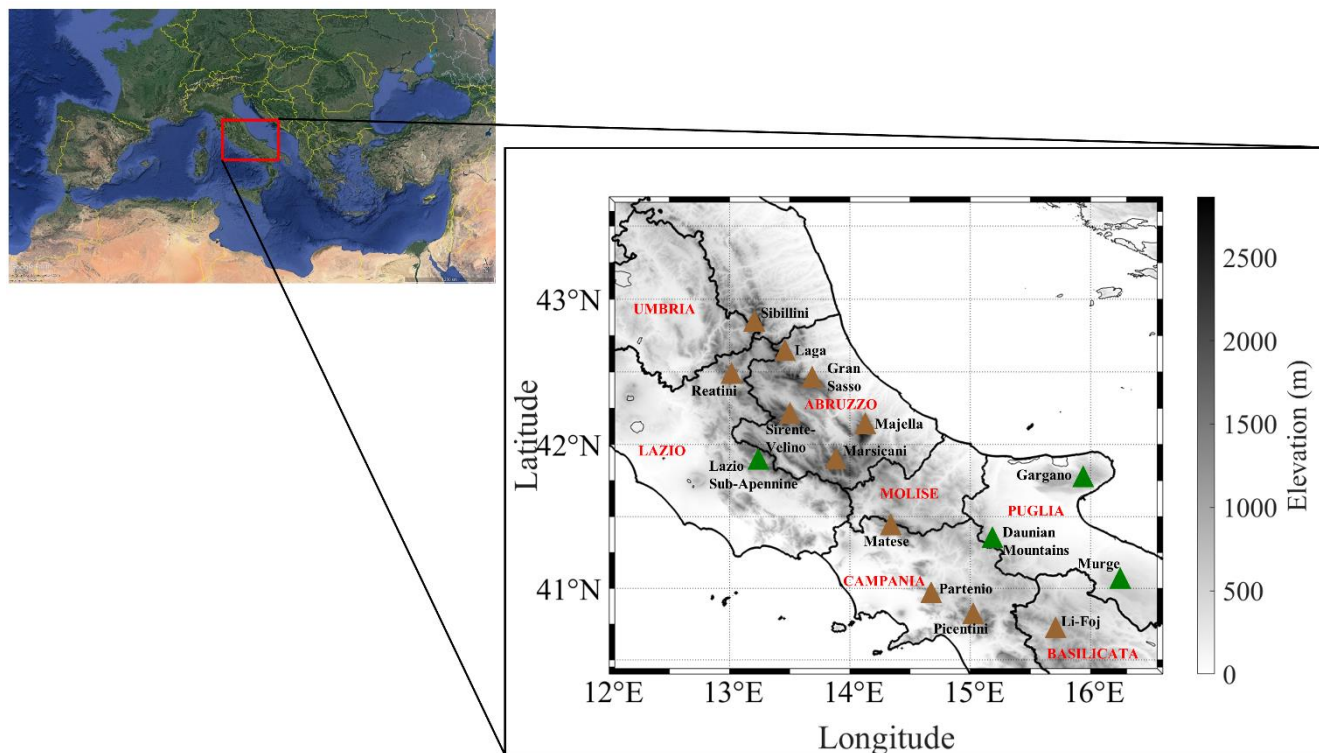
1040

1045

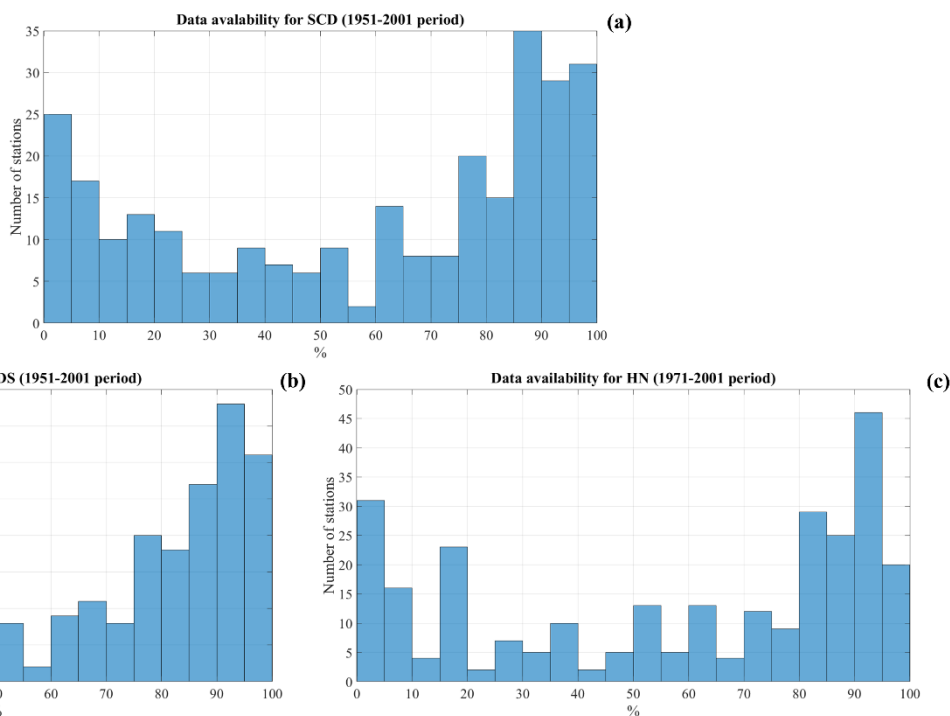
1050



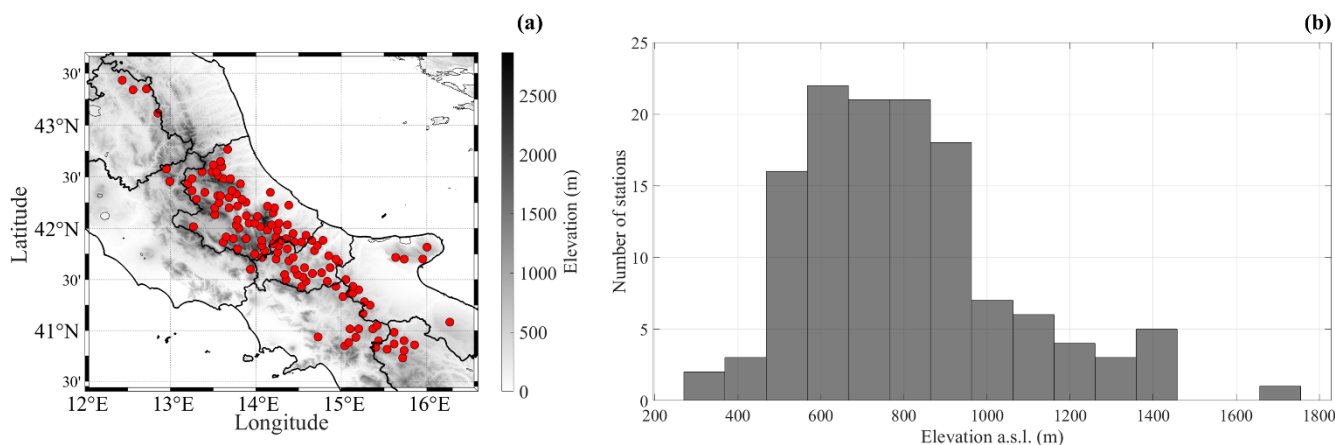
LIST OF FIGURES



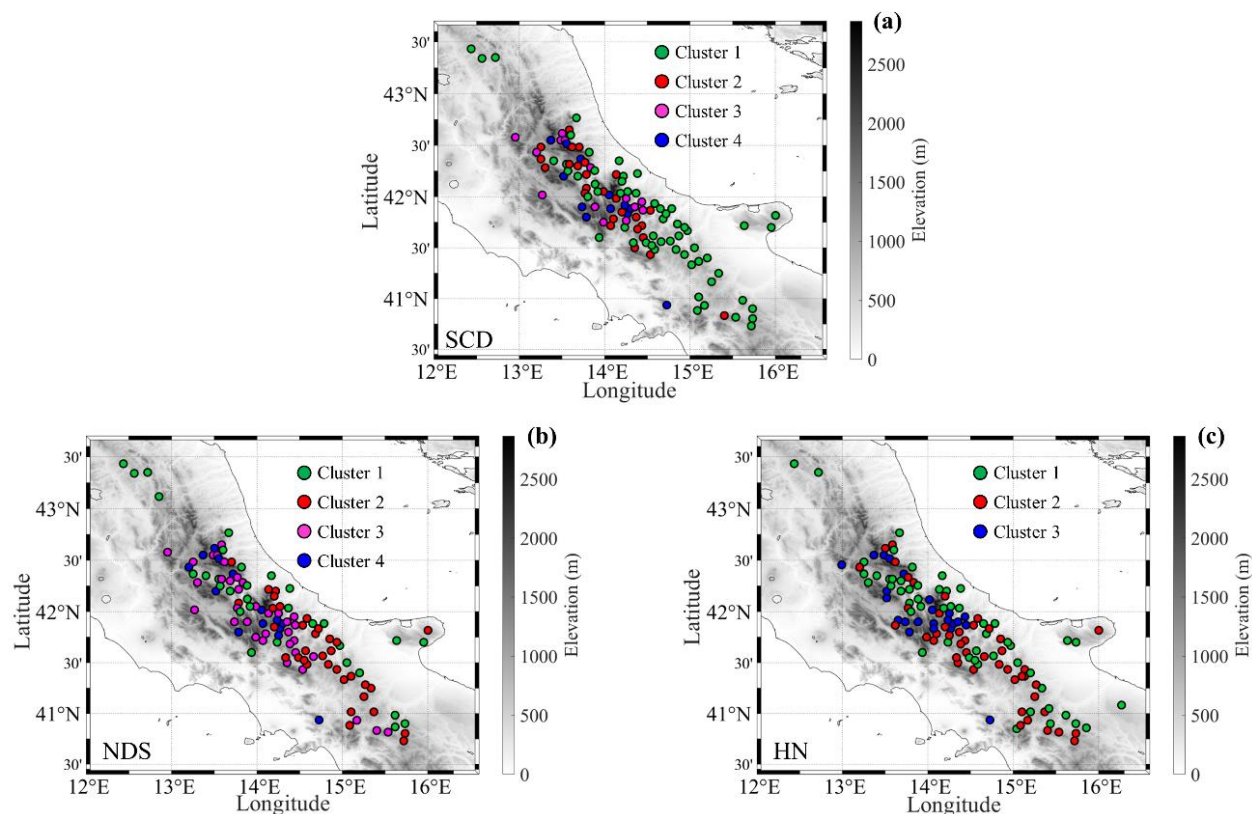
1055 **Figure 1:** In the left panel, a map of Mediterranean area, including the study region (highlighted as red solid-outlined box) is presented. The right panel shows a digital elevation model of the investigated area, with several mountain ranges mentioned in the main text. More specifically, the main Apenninic reliefs are marked as brown filled-in triangles, whereas the filled-in green triangles indicate several Apennine offshoots. The black line shows the boundaries of the Italian administrative regions included in the study area (the official name of the regions is indicated in red). Images credit: © Google Earth, Data Sio, NOAA, U.S. Navy, NGA, GEBCO.



1060 **Figure 2: Histogram of the data availability (in %) for the considered snowfall parameters: SCD (a), NDS (b) and HN (c). Note that in this figure all rescued stations have been considered.**



1065 **Figure 3: Panel (a) shows the location of the stations (129 in total) considered for the analyses carried out in this work. The black line shows the boundaries of the Italian administrative regions included in the study area. Panel (b) sketches the number of available stations per elevation.**



1070

Figure 4: Clustering of stations based on monthly data of SCD (a), NDS (b) and HN (c). The stations are color-coded according to the cluster memberships.

1075

1080

1085

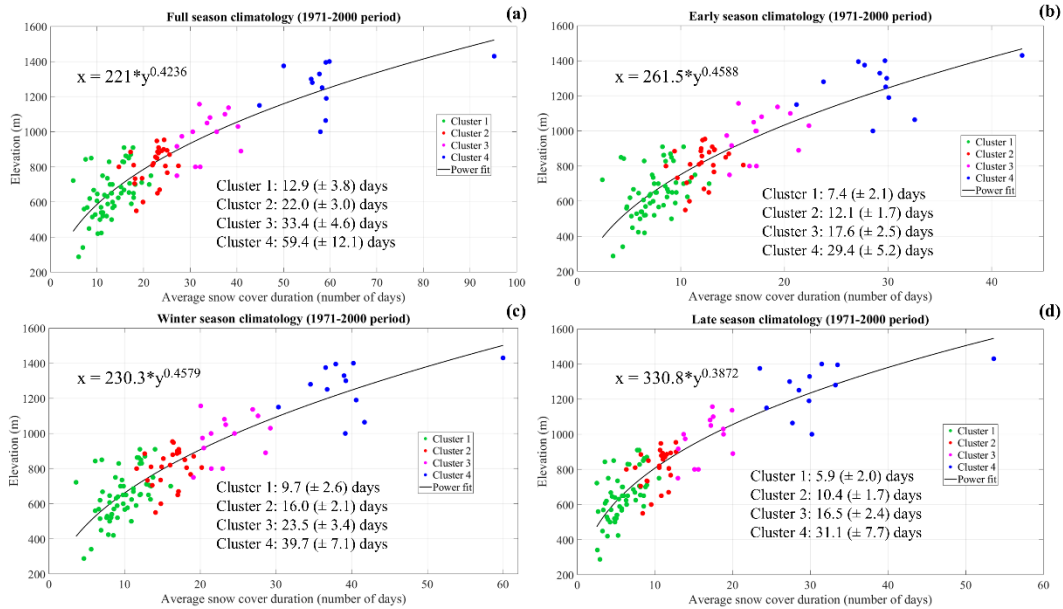


Figure 5: Climatology of snow cover duration (SCD) for (a) full, (b) early, (c) winter and (d) late season. Average values are for the period 1971-2000. Each point represents a station that is color-coded according to the membership cluster. The black solid line represents the power fit. The text boxes show the power fit equation and the average and standard deviation values for each cluster.

1090

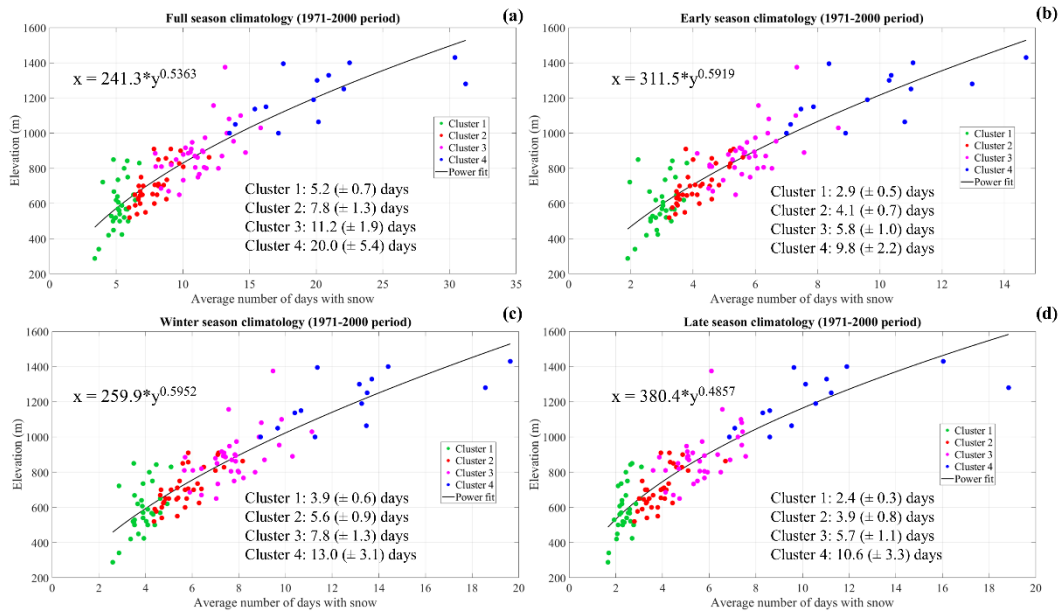


Figure 6: Climatology of number of days with snow (NDS) for (a) full, (b) early, (c) winter and (d) late season. Average values are for the period 1971-2000. Each point represents a station that is color-coded according to the membership cluster. The black solid line represents the power fit. The text boxes show the power fit equation and the average and standard deviation values for each cluster.

1095

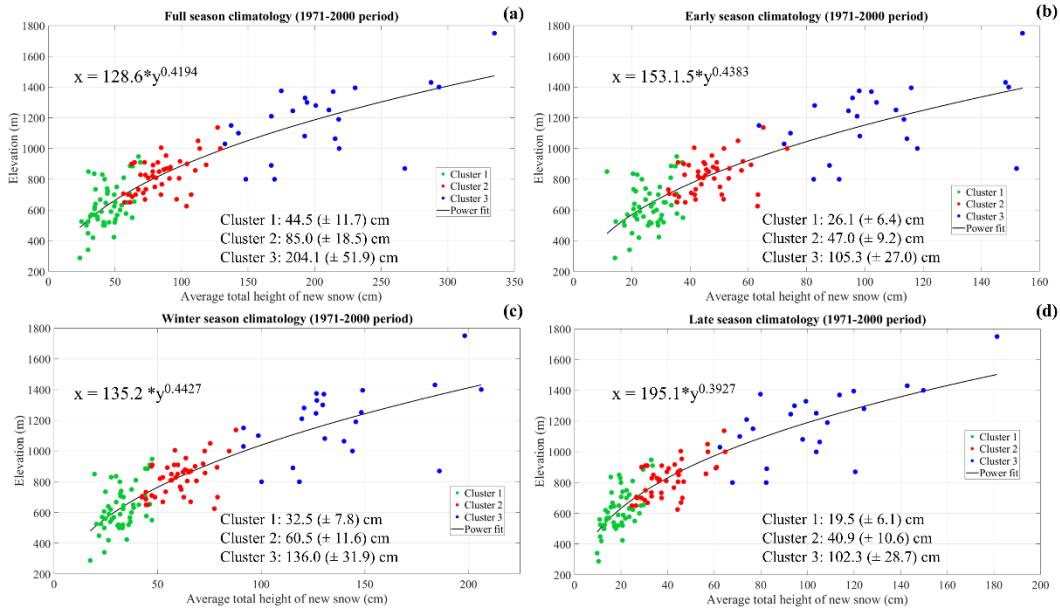


Figure 7: Climatology of height of new snow (HN) for (a) full, (b) early, (c) winter and (d) late season. Average values are for the period 1971-2000. Each point represents a station that is color-coded according to the membership cluster. The black solid line represents the power fit. The text boxes show the power fit equation and the average and standard deviation values for each cluster.

1100

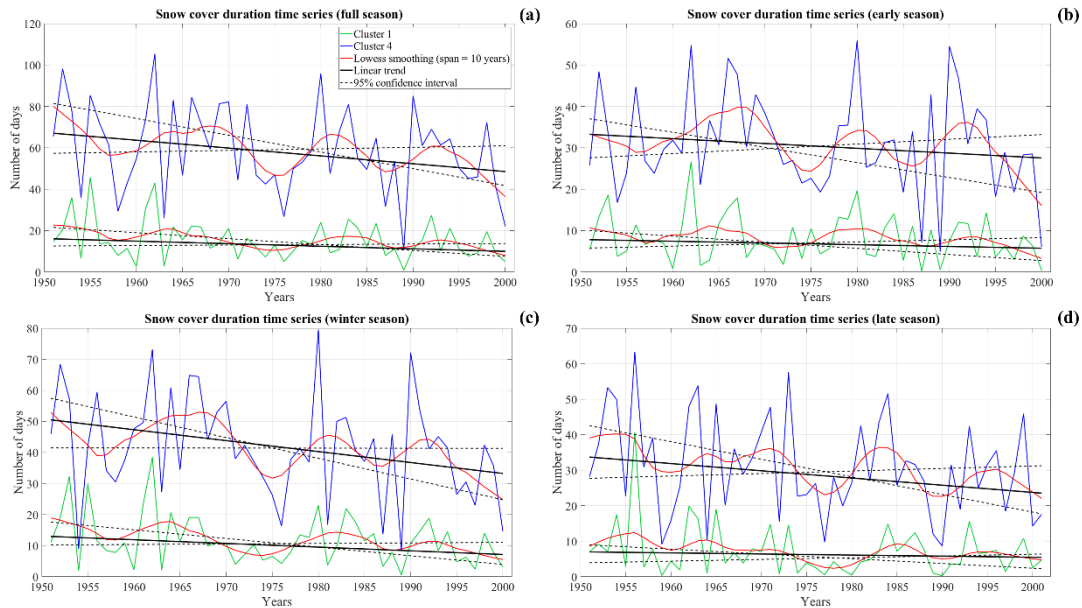


Figure 8: Cluster 1 (green line) and cluster 4 (blue line) snow cover duration (SCD) time series for full (a), early (b), winter (c) and late (d) season. The black solid line shows the linear trend, the dashed black line the 95% confidence interval for linear trend, whereas the red line marks the lowess smoothing (span = 10 years). The period from 1951 to 2001 has been considered.

1105

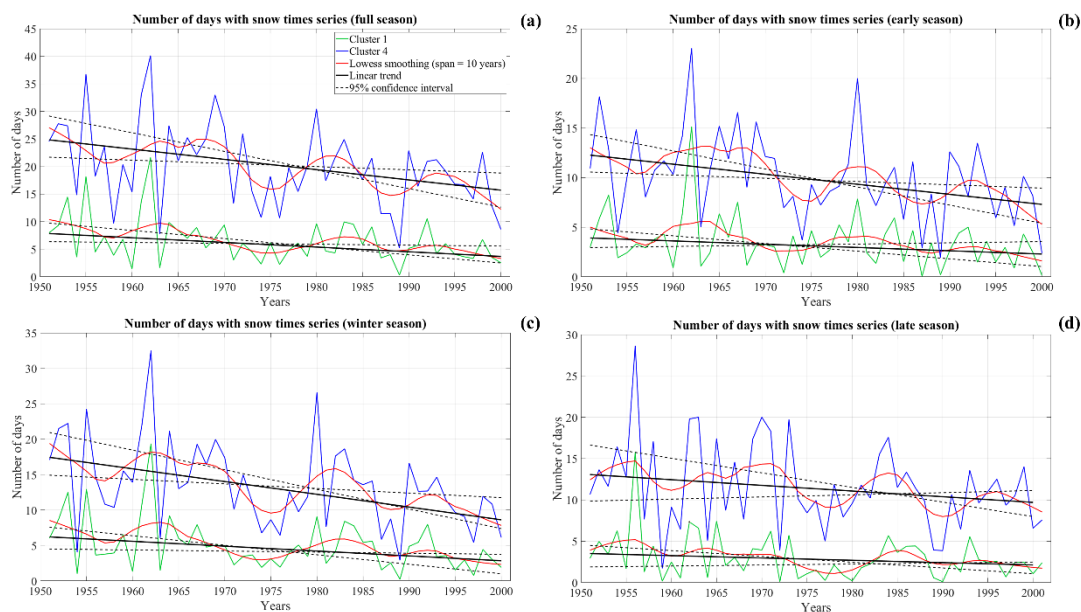


Figure 9: Cluster 1 (green line) and cluster 4 (blue line) number of days with snow (NDS) time series for full (a), early (b), winter (c) and late (d) season. The black solid line shows the linear trend, the dashed black line the 95% confidence interval for linear trend, whereas the red line marks the lowess smoothing (span = 10 years). The period from 1951 to 2001 has been considered.

1110

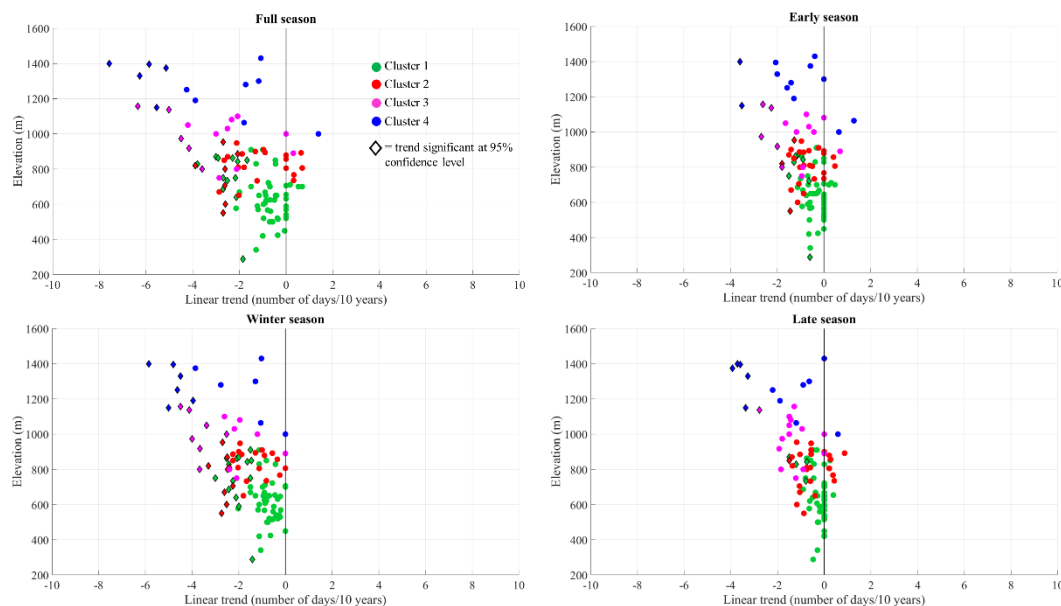


Figure 10: Seasonal snow cover duration (SCD) trends (expressed as number of days/10 years) as function of elevation. Each point represents one station and is color-coded according to the membership cluster. Trends significant at 95% confidence level are displayed as diamond marker.

1115

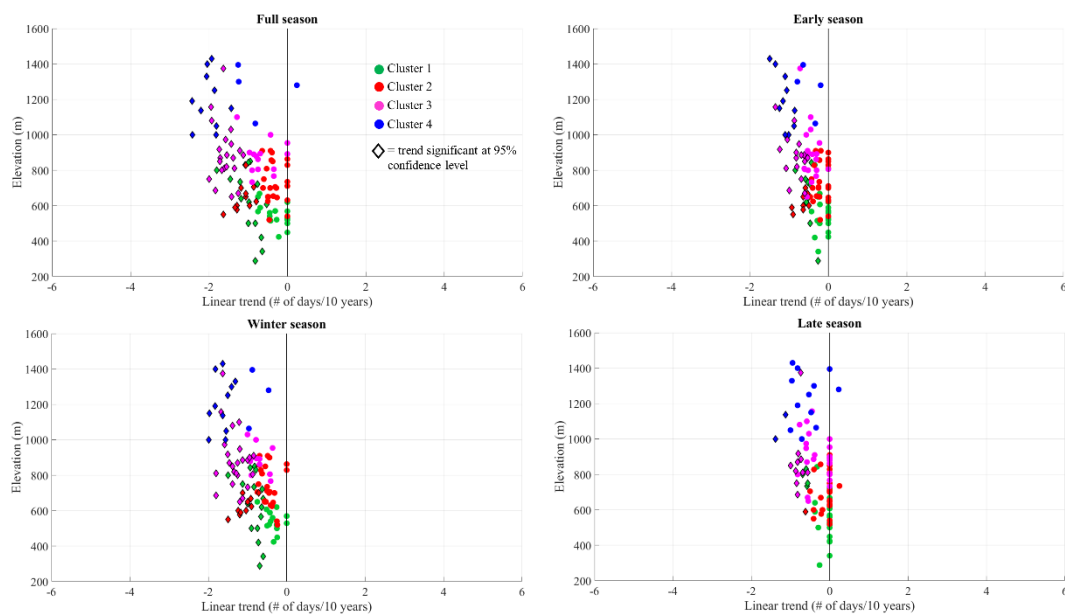
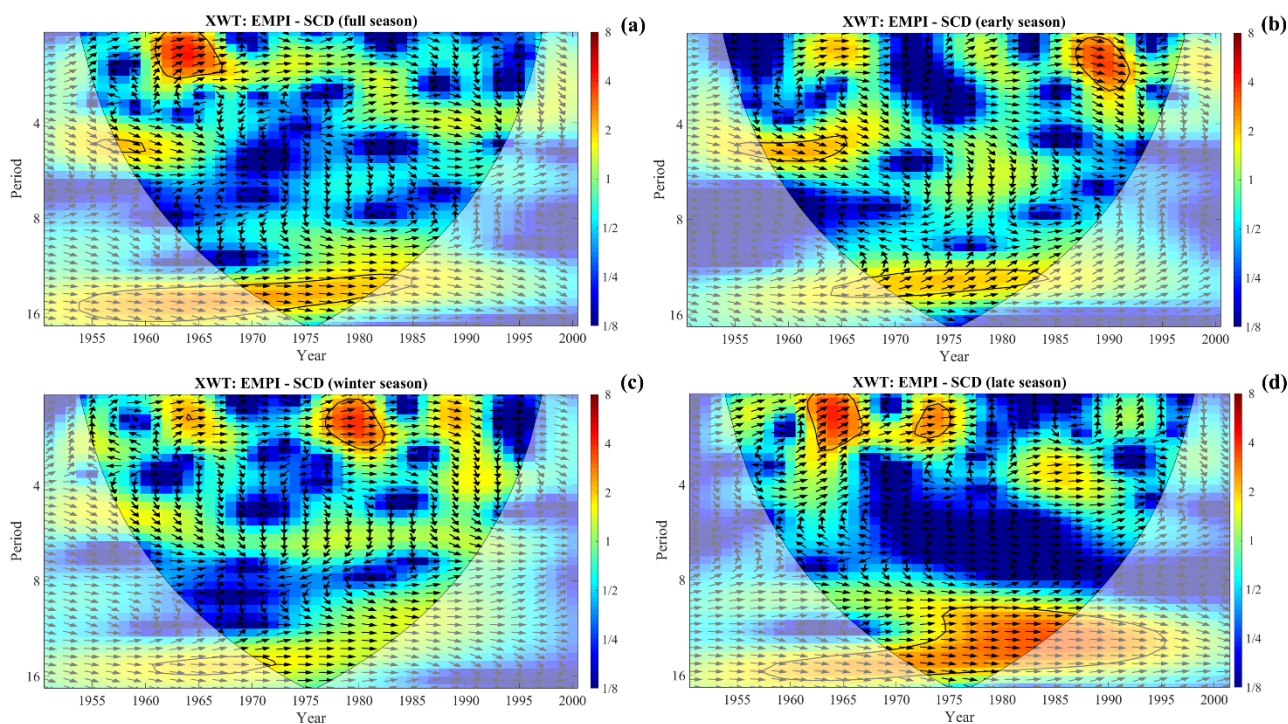
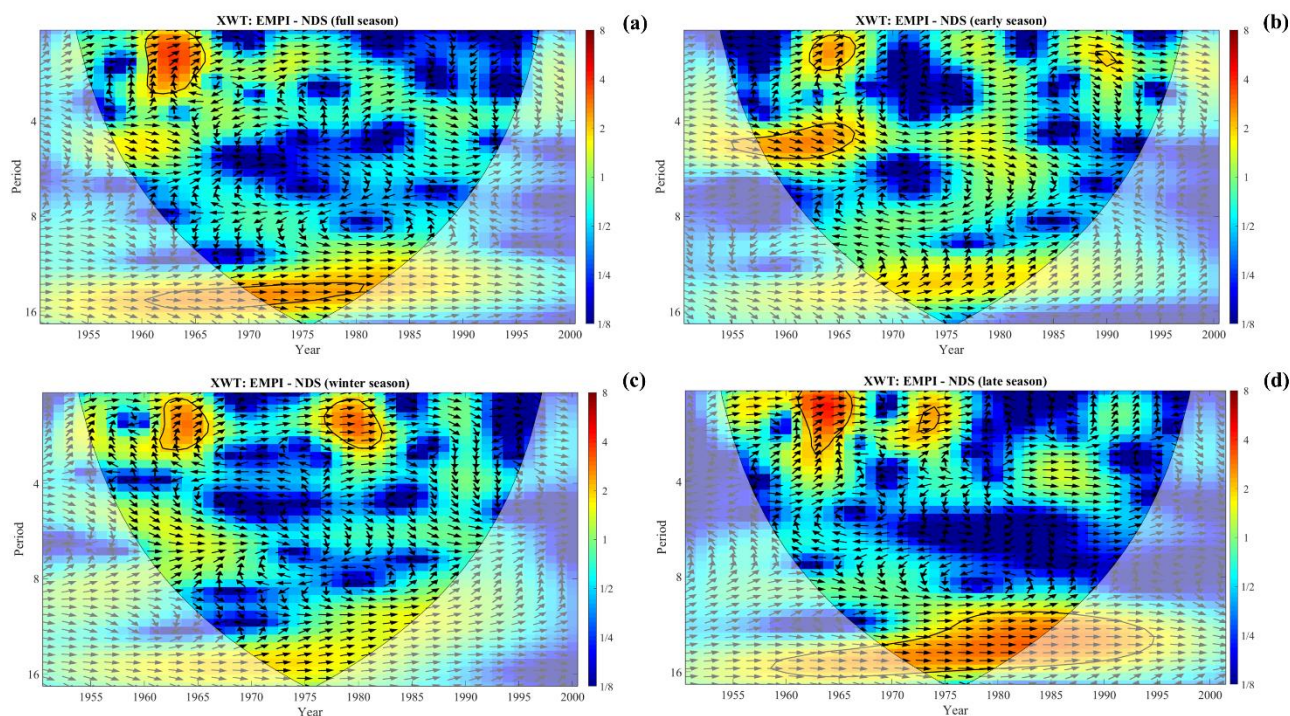


Figure 11: Seasonal number of days with snow (NDS) trends (expressed as number of days/10 years) as function of elevation. Each point represents one station and is color-coded according to the membership cluster. Trends significant at 95% confidence level are displayed as diamond marker.



1125 **Figure 12: Cross Wavelet Transform (XWT) between Eastern Mediterranean Pattern Index (EMPI) and the cluster 4 snow cover duration (SCD) time series for (a) full season, (b) early season, (c) winter season, and (d) late season. The black arrows indicate the phase relationship between the respective time series. The thick contour designates the 5% significance level against red noise; the cone of influence, where edge effects might distort the picture, is shown as a lighter shade. All XWT spectra refer to the period 1951-2001.**

1130



1135

Figure 13: Cross Wavelet Transform (XWT) between Eastern Mediterranean Pattern Index (EMPI) and the cluster 4 number of days with snow (NDS) time series for (a) full season, (b) early season, (c) winter season, and (d) late season. The black arrows indicate the phase relationship between the respective time series. The thick contour designates the 5% significance level against red noise; the cone of influence, where edge effects might distort the picture, is shown as a lighter shade. All XWT spectra refer to the period 1951-2001.